

A TRIDENT SCHOLAR PROJECT REPORT

NO. 257

A Side Scan Sonar and
Sub-Bottom Profiler Study
Over Buried River Channels,
Chesapeake Bay



19990122 080

UNITED STATES NAVAL ACADEMY
ANNAPOLIS, MARYLAND

This document has been approved for public
release and sale; its distribution is unlimited.

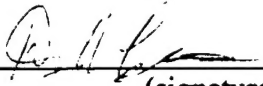
REPORT DOCUMENTATION PAGE			Form Approved OMB no. 0704-0188	
<small>Public reporting burden for this collection of information is estimated to average 1 hour of response, including the time for reviewing instructions, searching existing data sources, gathering and maintaining the data needed, and completing and reviewing the collection of information. Send comments regarding this burden estimate or any other aspect of this collection of information, including suggestions for reducing the burden, to Washington Headquarters Service, Directorate for Information Operations and Reports, 1215 Jefferson Avenue, Washington, DC 20540-6011.</small>				
1. AGENCY USE ONLY (Leave blank)		2. REPORT DATE		3. REPORT TYPE AND DATES COVERED
4. TITLE AND SUBTITLE A side scan sonar and sub-bottom profiler study over buried river channels, Chesapeake Bay				5. FUNDING NUMBERS
6. AUTHOR(S) Dewey A. Lopes				
7. PERFORMING ORGANIZATIONS NAME(S) AND ADDRESS(ES) U.S. Naval Academy, Annapolis, MD				8. PERFORMING ORGANIZATION REPORT NUMBER USNA Trident report; no. 257 (1998)
9. SPONSORING/MONITORING AGENCY NAME(S) AND ADDRESS(ES)				10. SPONSORING/MONITORING AGENCY REPORT NUMBER
11. SUPPLEMENTARY NOTES Accepted by the U.S. Trident Scholar Committee				
12a. DISTRIBUTION/AVAILABILITY STATEMENT This document has been approved for public release; its distribution is UNLIMITED.				12b. DISTRIBUTION CODE
13 ABSTRACT (Maximum 200 words) This study used a sub-bottom profiler and side-scan sonar to study the most recent Holocene channels in the mid-Chesapeake Bay near Annapolis, MD. Nearly two dozen transects collected approximately 150 km of sub-bottom and 90 km of side scan data. Analysis of the sub-bottom data suggests three strong sub-bottom returns separate four sub-bottom layers. They are found at depths between 1.5m and 14m below the sediment/water interface. Channels cut into some of these layers have a north-south orientation. Analysis of the side scan data and bathymetric profiles indicates that the orientation of the sub-bottom layering tends to follow the general bottom surface bathymetry and orientation of the present channel. Bottoms surface morphology does not appear to reflect sub-bottom characteristics. Both side scan and sub-bottom data reflect sediment deposition. Sedimentation in the study area, south of the turbidity maximum in the Chesapeake Bay, is approximately 0.05 cm/yr to 0.075 cm/yr. This estimate uses the measured layer thickness and assumes that the deepest sub-bottom return separating the two deepest layers represents the 18,000 year old Cape Charles paleochannel. This seems plausible since the layering conforms to the depth and location of the Cape Charles paleochannel previously determined.				
14. SUBJECT TERMS Chesapeake Bay, sedimentation, paleochannels, geologic-history, side scan sonar, sub-bottom profiler				15. NUMBER OF PAGES
				16. PRICE CODE
17. SECURITY CLASSIFICATION OF REPORT	18. SECURITY CLASSIFICATION OF THIS PAGE	19. SECURITY CLASSIFICATION OF ABSTRACT	20. LIMITATION OF ABSTRACT	

U.S.N.A. – Trident Scholar project report; no. 257 (1998)

**A Side Scan Sonar and Sub-Bottom Profiler Study Over Buried River Channels,
Chesapeake Bay**

by

Midshipman Dewey A. Lopes, Class of 1998
United States Naval Academy
Annapolis, Maryland


(signature)

Certification of Advisor Approval

Associate Professor Peter L. Guth
Department of Oceanography


(signature)

4 MAY 1998
(date)

Acceptance for the Trident Scholar Committee

Professor Joyce E. Shade
Chair, Trident Scholar Committee


(signature)

4 May 1998
(date)

USNA-1531-2

Abstract

This study used a subbottom profiler and side-scan sonar to study the most recent Holocene channels in the mid Chesapeake Bay near Annapolis, MD. Nearly two dozen transects collected approximately 150 km of sub-bottom and 90 km of side scan data.

Analysis of the sub-bottom data suggests three strong sub-bottom returns separate four sub-bottom layers. They are found at depths between 1.5m and 14m below the sediment/water interface. Channels cut into some of these layers have a north-south orientation. Analysis of the side-scan data and bathymetric profiles indicates that the orientation of the subbottom layering tends to follow the general bottom surface bathymetry and orientation of the present channel. Bottom surface morphology does not appear to reflect sub-bottom characteristics.

Both sidescan and subbottom data reflect recent sediment deposition. Sedimentation in the study area, south of the turbidity maximum in the Chesapeake Bay, is approximately 0.05 cm/yr to 0.075 cm/yr. This estimate uses the measured layer thicknesses and assumes that the deepest subbottom return separating the two deepest layers represents the 18,000 year old Cape Charles paleochannel. This seems plausible since the layering conforms to the depth and location of the Cape Charles paleochannel previously determined.

Key words: Chesapeake Bay, sedimentation, paleochannels, geologic-history, side-scan-sonar, subbottom-profiler

Table of Contents

Abstract	1
List of Figures.....	3
Introduction.....	4
Background	6
GEOLOGY	6
SEDIMENTATION	8
SIDE SCAN SONAR.....	12
SUB-BOTTOM PROFILER	16
Methods	20
DATA COLLECTION	21
DATA ANALYSIS	25
Results and Discussion	29
SUBBOTTOM LAYERING.....	29
LOCATING THE PALEOCHANNELS	29
ORIENTING THE LAYERING	37
CLASSIFYING THE PALEOCHANNEL.....	38
BOTTOM BATHYMETRY	40
SEDIMENTATION RATES	45
Conclusions.....	45
NAVAL APPLICATIONS.....	47
Acknowledgements	50
References Cited.....	51
APPENDIX A: Using Cap'n Navigation Program.....	55
APPENDIX B: Using Chirps	56
APPENDIX C: Useful CHIRPS Information	58
APPENDIX D: Using NOVA Software	64

List of Figures

Figure 1 Paleochannels located by Coleman et al., 1990.....	7
Figure 2 Side scan sonar beam pattern.....	14
Figure 3 Side scan sonar and sub-bottom profiler data coverage.....	17
Figure 4 Preliminary search area and detailed study area.....	21
Figure 5 A typical side scan sonar sonograph.....	25
Figure 6 Side scan sonar mosaic.....	26
Figure 7 Typical sub-bottom profiler image.....	27
Figure 8 Transect B showing sub-bottom layers I, II, III, and IV.....	30
Figure 9 Chart showing the transects that identify and orient the deepest sub-bottom layering.....	31
Figure 10 Transect A showing layers I, II, and III. Width of record approximately 300 m.....	31
Figure 11 Transect C showing layers I, II, III, and IV.....	32
Figure 12 Transect D showing layers I, II, III, and IV.....	33
Figure 13 Transect E showing layers I, II, III, and IV.....	34
Figure 14 Transect F showing layers I, II, III, and IV.....	34
Figure 15 Transect Y showing layers I, II, III, IV, and the location of the channel 'C'.....	35
Figure 16 An enlarged view of the deep layer from transect Y.....	36
Figure 17 Transect Z showing layers I, II, III, and IV.....	36
Figure 18 Transects C (blue) and E (green) cross with transects Z (skewed on the left) and Y (skewed on the right).....	37
Figure 19 Sub-bottom profile of section F from Colman and Halk, 1989b.....	39
Figure 20 Bathymetric map of the study area.....	41
Figure 21 Sub-bottom profile across the northern edge of the bathymetric map.....	42
Figure 22 Side scan mosaic with two crossover sub-bottom profiles (transects X and Z).....	43
Figure 23 Side scan mosaic and concurrent sub-bottom profile.....	44

Introduction

The Chesapeake Bay is currently one of Maryland's most valuable resources. It is a plentiful source of marine organisms and has many industrial and recreational uses. The morphology of the Chesapeake Bay is very complicated. In the last major glaciation, sea level dropped 85 m on the mid-Atlantic continental shelf (Dillon and Oldale, 1978; Bloom, 1983), exposing the area occupied by the Chesapeake Bay. During this period, the Susquehanna River system cut a deep valley into the coastal plain. Rising sea levels, following the glacial period, transformed the river valley into the contemporary open-bay estuary (Colman and Hobbs, 1987, 1988; Colman and Halka, 1989a, 1989b). Today, the bay evolution continues as estuarine sediments fill the fluvial channel (Colman et al., 1990).

Many tools can be used to help study the sea floor, including the side-scan sonar, and the sub-bottom profiler. These are both acoustic data collection methods. The side-scan sonar can be used to help characterize the consistency and morphology of the sea floor (Symonds and Davies, 1986). The sub-bottom profiler, however, gives insight to the sediments and layers beneath the sea floor (Schock and LeBlanc, 1990). In both cases, the raw data alone will not provide images that can be easily viewed for analysis. Digital image processing techniques must first be applied to the data. Implementing these processes leads to enhanced sonar images.

This project uses side-scan sonar data, sub-bottom profiler data, and digital image processing techniques to create images of the bay floor and its corresponding sub-bottom. By correlating these images, it is possible to create a three dimensional mosaic of the bay

floor. This mosaic contains the contours and characteristics of the bay-floor, as well as the location and characteristics of sediments found in the sub-bottom.

Previously, small scale seismic surveys have covered the entire Bay area and documented a series of three old channels from the last ice age (Colman et al., 1990). This study focuses on a small area near Kent Island, Maryland, approximately 10 km east of Annapolis, Maryland. The end result of this study is to decipher the recent geologic history of the study area. Using the digital mosaics, it is possible to determine the relationship between the bottom surface topography and the sub-bottom layering. It is also possible to determine sediment fluxes. This includes both the changes in the characteristics of the sediments and the rate of sedimentation in the area. This will prove the existence of the most recent Cape Charles Paleochannel and show how it has changed over time. This will help provide clues to the long-term development of the Chesapeake Bay.

Due to its growing number of uses, it is essential to know how the bay develops over time. Consideration of site 104 (located just north of the Annapolis-Kent Island Bridge) for the placement of 4.6 million cubic meters of dredged material is a major environmental concern (U.S. Army Corps of Engineers, 1998). The location of site 104 is near the head of the Chesapeake Bay estuary. This is significant because the head of the estuary contains the turbidity maximum. This is the zone where river discharge meets the estuary causing unusually high rates of sediment deposition (Zabawa, 1978). Identifying patterns of sedimentation and bottom surface morphology in the northern part of the

Chesapeake Bay will help determine whether it is geologically safe to place dredge spoils in site 104.

Background

The study has four main objectives: 1) locate sub-bottom layering to determine the location of the Susquehanna River paleochannels; 2) determine the orientation of the paleochannels; 3) determine if there is a correlation between sub-bottom layering and bottom surface bathymetry; and 4) determine sedimentation rates over the paleochannels.

Geology

The Chesapeake Bay is one of the largest open bay estuaries in the world. It is approximately 300 km long and is 48 km at its widest point (Hill and Halka, 1989). The Susquehanna River is the largest of the six tributaries, and supplies the most sediment to the bay (Gross et al., 1978). The modern bay formed due to a rising sea level after the last major glacial period. At the height of the glacial period, the Susquehanna River had carved a deep river valley into the coastal plain. The river valley was subsequently drowned as the glaciers receded (Oertel and Foyle, 1995). The cyclic nature of glacial periods and the bay's prominent central channel suggest the Susquehanna has eroded multiple paleochannels beneath the Chesapeake Bay.

Three major paleochannels have been located and studied, from oldest to youngest, the Exemore, Eastville, and Cape Charles paleochannels (see figure 1). All three paleochannels correspond to major low-stand events during the Quaternary (Chen et al., 1995). They vary in age and location, but share some common characteristics. The

paleochannels migrated towards the southwest. As a result, the older paleochannels generally do not cross westward of a younger one. Also, in the northern part of the bay, the three channels tend to be very close together, spreading out as they reach the mouth of the bay.

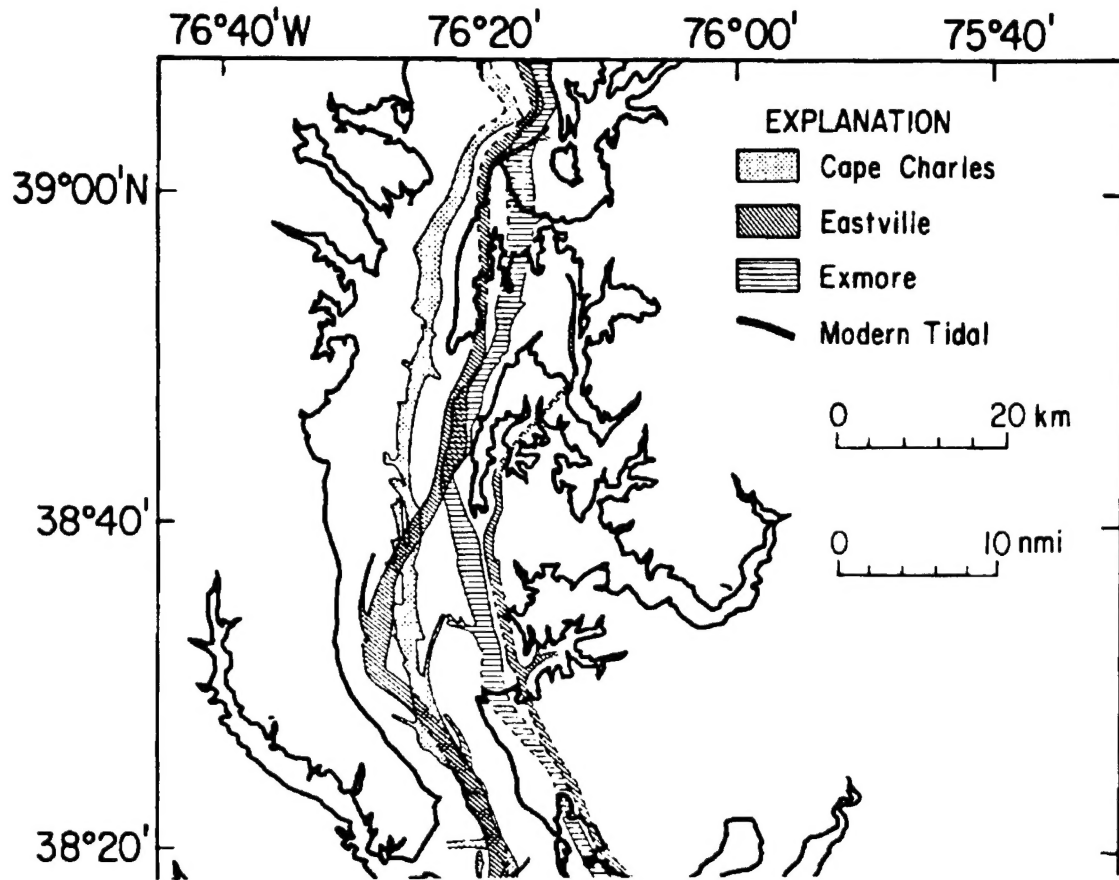


Figure 1 Paleochannels located by Coleman et al., 1990.

The Cape Charles paleochannel is the youngest, associated with the most recent glaciation during the late Wisconsinian (18ka). For the most part, it is located near the central channel of the bay. There are some areas, however, where the paleochannel is offset from the bathymetric channel (Colman et. al, 1990). Examples include the region

south of the Potomac River (Colman and Hobbs, 1988; Colman and Halka, 1989) and the mouth of the bay, where the central axis of the current bay has been shifted some 12 km south of the Cape Charles paleochannel.

The Eastville paleochannel is of intermediate age. It is presumed to correlate to the preceding glacial period dating it near 150 ka (Colman and Mixon, 1988). It runs along the eastern edge of the Chesapeake Bay. It passes beneath Kent Island in the northern part of the bay. The Eastville paleochannel briefly crosses westward of the younger Cape Charles paleochannel near Calvert Cliffs (Colman et. al, 1990). It then continues southward along the eastern shore until it curves sharply eastward, passing underneath the Delmarva Peninsula near Eastville, MD.

The Exemore paleochannel is the oldest. It is most likely to correlate to oxygen isotope stage 8 (270 ka) or stage 12 (430 ka). It is located underneath the western edge of the Delmarva Peninsula. It never crosses the Eastville paleochannel. In the northern part of the bay, it runs east of Kent Island. It eventually crosses the Delmarva Peninsula near Exemore, MD.

Sedimentation

Based on a variety of methods, many studies describe the sedimentation rates for the Chesapeake Bay (Table 1). The net sedimentation rate is the difference between the rate of deposition and the rate of erosion of sediments. A sedimentation rate is the net rate at which sediment accumulates in a given area. Sedimentation rates vary depending

on the sediment type, and the physical characteristics (water depth, current, bathymetry, etc.) of the observation area.

Table 1 Previous studies of Chesapeake Bay sedimentation.

Study	Process	Deposition Rate	Erosion Rate	Sedimentation Rate
Schubel and Carter, 1977	Single Segment Box Model (Sediment Budget)	—	—	0.08 cm/yr —
Kerhin et al., 1982	Sediment Budget	0.76 cm/yr	0.69 cm/yr	0.07 cm/yr
Kerhin et al., 1988	Sediment Budget	0.84 cm/yr	0.64 cm/yr	0.20 cm/yr
	Pb210	0.71 cm/yr	—	—
Officer et al., 1984	Pb210	0.76 cm/yr	—	—

Sediment budgets are the most common means for determining the sedimentation rates in the bay. Sediment budgets determine the sediment fluxes for an area, and then correlate the flux to the size of the area to ascertain a sedimentation rate. More accurate sedimentation rates, however, come from geochemical tracing from sediment core samples.

A sediment budget is a simple way to determine the net sediment change in an area. A sediment budget accounts for all sources and sinks of sediment. Sources of sediment include river output, shore erosion, ocean sediments, and biologic decay, while sinks include suspended matter, erosion, and discharge. The fluxes of sediment are added together to determine the rate of change of sediment for the area. Fluxes are typically calculated by measuring flow rates and suspended sediment concentrations (Dyer, 1986).

Geochemical tracing is a very complicated process. In general, geochemical tracing monitors and measures the radioactivity of a trace element (Pb210 in this case). The Pb210 isotope can determine particle mixing and sediment accumulation rates

(Cochran, 1984). By measuring the amount of the lead isotope and the associated levels of radioactivity, it is possible to determine the sediment accumulation rates of the core sample area.

One of the earliest estimates of sedimentation rates in the Chesapeake Bay was completed in 1977. Schubel and Carter (1977, cited in Dyer 1986) used a single segment box model to model the sediment fluxes for the Chesapeake Bay. Using an average input of 1.89×10^6 tons of sediment per year, they assumed 92% of the sediment was deposited on the bay floor, while the remaining 8% stayed in the water column. As with most sediment budgets, the deposition rates are derived from actual dredging rates (Dyer, 1986). A dredging rate is calculated using the volume of sediment dredged from a particular area and the time necessary to naturally refill the area. Using this method, they calculated a sedimentation rate of 0.08 cm/yr (Dyer, 1986).

Kerhin et al. (1982) computed a similar rate. Using a sediment budget with average deposition and erosion rates they calculated a net deposition of 0.07 cm/yr for the Chesapeake Bay (Kerhin et al, 1982). Six years later, Kerhin et al. (1988) compared the sedimentation rates from sediment budgets to those determined through geochemical tracing. Using an updated sediment budget, they determined the average rate of deposition for the entire bay to be 0.84 cm/yr, and the average rate of erosion to be 0.64 cm/yr. This gives a net sedimentation rate of 0.20 cm/yr (Kerhin et al., 1988).

Analysis of sediment core samples using Pb210 as a tracer gave a deposition rate of 0.71 cm/year (Helz et al. 1981). This is comparable to the deposition rate of 0.84 cm/yr determined by Kerhin et al. (1988) using the sediment budget because sedimentation

estimates based on Pb210 do not include erosion (Kerhin et al., 1988). Applying the rate of erosion to the Pb210 rate would give a net sedimentation rate of 0.07 cm/yr. This figure is identical to that determined by Kerhin et al. (1982), and similar to that by Schubel and Carter (1977, cited in Dyer, 1986).

Officer et al. (1984) calculated two sedimentation rates from geochemical tracing. By taking a straight average of the Pb210 rates calculated for different core samples, they computed an average deposition rate of 0.76 cm/yr (this includes all sediment types found in the bay averaged over the entire area of the bay). By comparing the optimum mass sedimentation rate with the straight average mass sedimentation rate of Pb210 traces, they determined the optimum sedimentation rate to be about half of the average sedimentation rate (0.38 cm/yr). The estimate from Pb210 data does not include subsidence. They suggest a subsidence rate correction of 0.3 to 0.7 cm/yr to bring the two sedimentation rates closer together.

Subsidence is similar to the leveling of a 'see-saw'. During the last glacial stage, the crust adjusted to the weight of the glaciers. As a result, some areas experienced uplifting (rising) while other areas experienced subsidence (sinking). When the glaciers recede, the balance must be restored. The Chesapeake Bay is subsiding due to post glacial rebound. The tide gauge record in Annapolis, MD, suggests a subsidence rate of 0.09 cm/yr (Nerem et al., 1998). Inspection of Nerem et al.'s (1998) data suggests the subsidence rate is near 0.1 cm/yr for all segments of the bay. This severely contradicts the subsidence rate suggested by Officer et al. (1984). The sedimentation rates derived by others are averaged over the entire bay. In reality, rates of sedimentation in different parts

of the bay vary greatly. The area of the bay from Turkey Point, MD, to Tolchester Beach, MD, has the highest rate of sedimentation in the Chesapeake Bay. The turbidity maximum is located in this area. It has the highest rate of sedimentation because it is the point in the bay where river output meets the relatively non-circulatory tidal water of the estuary (Zabawa, 1978). This increases the concentration of suspended sediments, causing higher sedimentation rates in the area.

Generally, the middle portion of the bay extending from the Annapolis-Kent Island bridge south to the Patuxent river is erosional. Its primary source of sediment is nearshore erosion (Dyer, 1986). This is a much smaller source than the river discharge present in the upper bay. In this region, deposition of sediments occurs mainly in the axial channel (Kerhin et al., 1988). This results in unusually low sedimentation rates compared to the rest of the bay. In contrast, the lower portion of the bay is depositional. It has moderate sedimentation rates compared to the middle portion of the bay. Since the study area covers the deep axial channel of the middle bay, one would expect to find low sedimentation rates.

Side Scan Sonar

A side scan sonar is a simple acoustic tool with many applications. Generally, it is used to determine the seafloor characteristics of a given study area. It emits sound pulses into the water column, and records the echoes from the different features. Applying basic geometric corrections and signal gains yields realistic images of the study area. These

images, called sonographs, are essentially oblique aerial views showing the shape and texture of the sea-bed (Symonds and Davies, 1986).

This study used the EG&G Model 260-TH Image Correcting Side Scan Sonar with a Model 300 digital tape unit and the EG&G Model 272-TD Dual Frequency Tow Fish. Most side scan sonar systems use two transducers, port and starboard. The transmitted energy has a wide vertical beam width and a narrow horizontal beam width. A narrow horizontal beam width means the energy will be transmitted along an axis perpendicular to the ship's track (the course of the ship through the water). A wide vertical beam width means there will be a continuous stream of data collected along each perpendicular axis from the ship's track to the maximum range (EG&G Marine Instruments, 1990).

The Model 272-TD transmits signals at 100 kHz (standard resolution) or at 500 kHz (high resolution). For geologic applications, the 100 kHz standard resolution is more useful. The actual operating frequencies for this resolution are $105 \text{ kHz} \pm 10 \text{ kHz}$. For this frequency, the tow fish transmits a 228 dB acoustic pulse, with 0.1 msec duration. The vertical beam width for the pulse is 50° , tilted down 20° , while the horizontal beam width is only 1.2° (EG&G Marine Instruments, 1990). This vertical beam width restricts the maximum range of the side scan sonar because it limits where the sound can travel (see figure 2).

The level of energy returned to the transducer (known as the echo level) is based on range, transducer beam pattern, grazing angle, hardness, and roughness of the sea floor. For the side scan sonar data to be useful, the raw amplitude of the tow fish data

must be manipulated through digital processing so the amplitude depends only on the backscattering strength or roughness of the sea floor. This digital processing applies several amplitude gains to the data. The 260-TH automatically applies some of these gains. However, only those corrections applied by the tow fish are reflected on the digital tape (EG&G Marine Instruments, 1991).

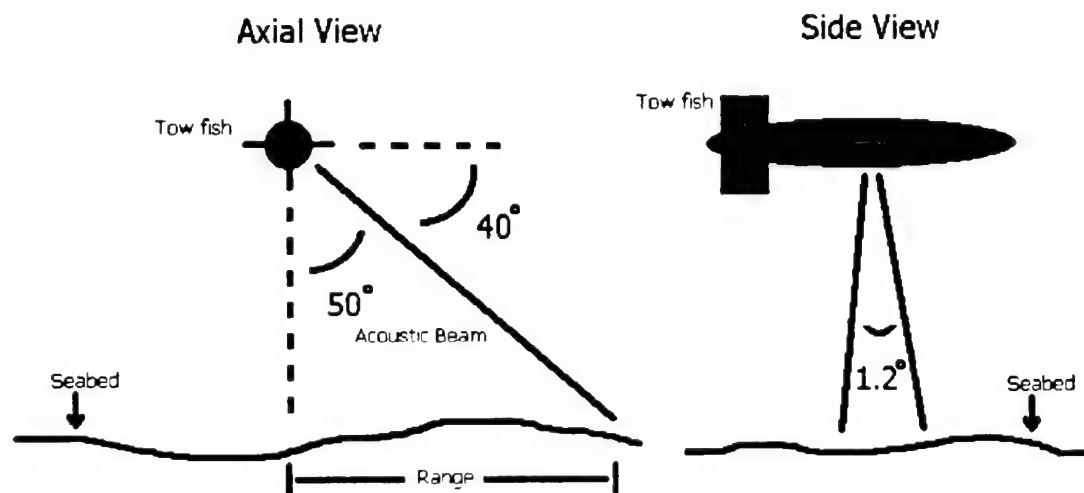


Figure 2 Side scan sonar beam pattern. The axial view of the side scan sonar tow fish shows the vertical beam width of the acoustic energy emitted. The side view of the tow fish shows the horizontal beam width. The range of the side scan sonar is a function of the vertical beam width.

Time varying gain (TVG) accounts for most of the data errors that arise from increasing range away from the ship's track. As sound propagates through water, it undergoes spreading and attenuation. The side scan sonar system accounts for this by applying an increasing gain to the amplitude of received signals with increasing travel times. This time varying gain is automatically applied by the Model 272-TD tow fish (EG&G Marine Instruments, 1990).

The angle of incidence at which the sonar beam strikes the sea floor also affects the amplitude of the return. When the angle of incidence is high (90°), all of the incident energy will be returned along the incident path. However, as the angle of incidence becomes smaller, the fraction of incident energy that is reflected back along the incident path decreases. Over a flat bottom, the angle of incidence will be highest near the ship's track, and will be lowest near the maximum range of the system. To account for this, the 260-TH automatically applies a gain to the back scattered signal which is not reflected in the recorded data. A low angle of incidence requires a larger gain (EG&G Marine Instruments, 1991). The angle varying gain removes the effects of both different grazing angles and an irregular beam pattern, both of which affect the angle at which the sonar beam strikes the sea floor.

The side scan data must also undergo a slant range correction. The signal received by the side scan sonar is a function of distance traveled (slant range). To view the data using the horizontal distance from the ship's track, the slant range correction is applied (Reed and Hussong, 1989). This is done at display time based on tow fish height computed from user input or automatic bottom tracking available on the 260-TH.

The final correction is a speed correction. The speed of the tow fish over ground varies due to ship's speed and current. As a result, the data is gathered at an irregular rate. The speed correction is applied to view the image with a square grid having uniform scale along the ship's track and an equal horizontal scale extending out to the selected range. The speed correction averages the ship's speed and plots the cross track profiles so the image has equal horizontal and vertical scales. The actual correction varies depending on

the selected range for the image, and displays some cross track profiles multiple times. This correction is applied at display time, for either user, speed log, or GPS input of the ship's speed.

The sampling rate of the side scan system depends on the range selected. Longer ranges have a lower sampling rate because the sound from the previous across track record takes longer to travel to maximum range and return. The lower sampling rate helps reduce interference. With a range of 100 m, the typical setting for this study, the sampling interval is every 0.150 second. The system stores 884 returns in each channel, with resolution decreasing with range. Each record contains 1800 bytes. This results in a data collection rate of 41.2 Mb/hour at 100 m range.

Sub-Bottom Profiler

The sub-bottom profiler uses a chirp sonar to produce images of sub-bottom sediments. It differs from side scan sonar in many respects. It uses a 'chirp' sonar system instead of a conventional sonar system. Further, the data images are vertical profiles of the sediments directly beneath the sub-bottom profiler, not horizontal images of the seabed (see figure 3). In this respect, the sub-bottom profiler is similar to a depth sounder but is designed to record sound penetration into the bottom.

The term chirp sonar refers to a high resolution sonar system designed to measure sediment properties while sub-bottom profiling (Schock et al., 1989). Using linear transmitting and receiving arrays, the chirp sonar emits a wide-band swept FM signal and measures the two way travel time of the signal (TWTT). The wide band-width is critical

because it provides the high resolution (10 cm) required to measure sediment properties while sub-bottom profiling (Schock et al., 1989).

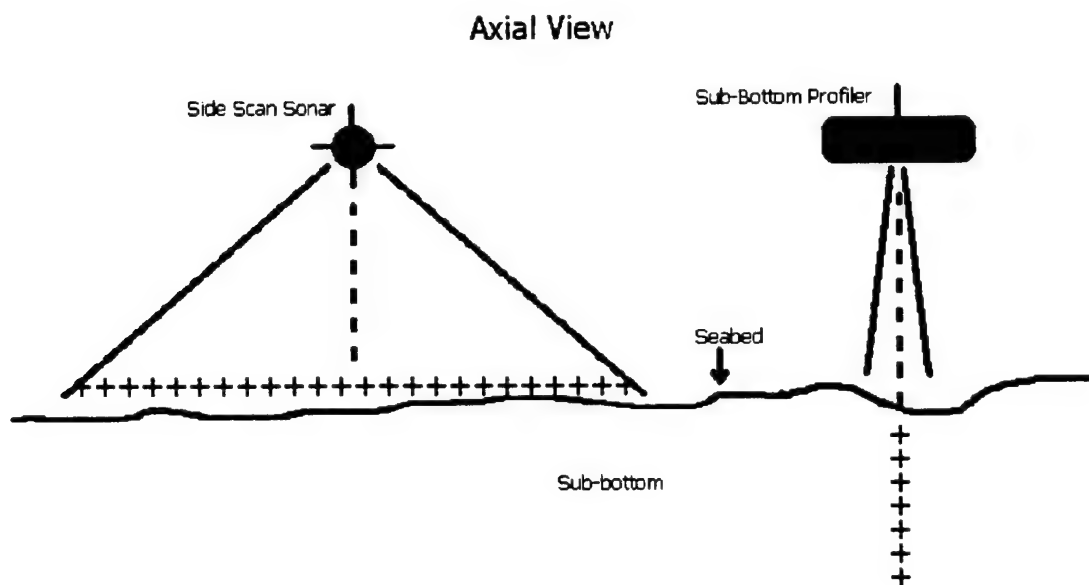


Figure 3 Side scan sonar and sub-bottom profiler data coverage. The side scan sonar covers the seabed surface area beneath the tow fish extending perpendicularly outwards from the axis of the tow fish (horizontal '+' line beneath the side scan sonar). The sub-bottom profiler data is the vertical profile of the sub-bottom sediments in a single line of data directly beneath the sub-bottom profiler (vertical '+' line beneath the profiler).

To produce an image, the chirp sonar must convert the measured TWTT into depths. This requires knowledge of the sound velocity, which varies slightly in water depending on temperature, salinity, and pressure, and significantly in rocks depending on lithification and pressure. For most applications involving shallow sediments (<100 m), such as this study, an assumed sound speed of 1500 m/second suffices for both the water and the water saturated unconsolidated sediments. The speed of 1500 m/second is the standard chosen and accepted in the field. All depth scales shown in this paper actually display TWTT converted to depth using this assumed sound speed.

This study used the EdgeTech X-StarPC Full Spectrum Sub-Bottom Profiler. It operates by transmitting FM pulses (4 kHz to 24 kHz, broken in separate ranges of 4 kHz to 14 kHz and 14 kHz to 24 kHz), and then measuring the intensity of returned pulses. The chirp sonar in the Full Spectrum system uses a digitally compressed FM signal. By compressing the signal, the signal-to-noise ratio of the acoustic image is maximized over the range of frequencies. This provides better images of the data because there is less "noise" mixed with the data (EdgeTech, 1996).

The Full Spectrum system has several other features characteristic of chirp sonar systems. First, it has separate transmitting and receiving arrays. By allowing simultaneous transmission and reception, this feature ensures the data is continuous. The acoustic data also has a gaussian shaped spectrum. This preserves the bandwidth of a pulse, even after the energy loss associated with attenuation from the sediment. Since the bandwidth remains virtually unchanged, the resolution of an attenuated pulse is almost the same as an un-attenuated pulse (EdgeTech, 1996).

The elimination of side lobes further enhances the data. Side lobes are essentially the edges of the transmitted signal. No useful data can be collected from the side lobes. This is accomplished by using a sweep frequency with a wide bandwidth (20°). Such a wide bandwidth smears potential side lobes together, and increases the number of return pulses for a given area. This increases the quality of the pulses received, and the resulting acoustic image (EdgeTech, 1996).

The subbottom profiler collects a data record every 0.28 seconds. For each frequency range, the system stores 1600 returns. With an assumed sound speed of 1500

m/second in the water column and the sediments, the 50 m record has a resolution of 3 cm. Navigation and other ancillary data bring the size of each record to 4176 bytes. The system collects 180 Mb/hr during operation.

Several digital processing techniques are used with the Full Spectrum system. The main method of adjusting the data is the time varying gain. Like the TVG with the side scan sonar, this applies an increasingly larger gain to acoustic pulses that travel greater distances to account for the natural attenuation associated with sound travelling through a medium. Unlike the side scan sonar, however, the user applies the TVG instead of the computer doing it automatically. This is because the two systems work in different media. The water column is the only medium that attenuates the side scan data. Since the water column is fairly uniform, the Model 260-TH can automatically apply the TVG to the side scan data for immediate viewing. The water column and sediments both attenuate the sub-bottom signal. Different sediments will affect attenuation differently, so the user needs greater control over the TVG.

The sub-bottom data can also be viewed by applying a straight gain. When this gain is applied, all of the data receive the same gain in intensity. This is done by multiplying the measured signal return strength of each data point collected by a constant. This essentially "darkens" the acoustic image at the time of display.

The last technique used to enhance the acoustic images of the sub-bottom profiler is changing the frequency of the modulated pulse. The Full Spectrum system has three frequency ranges: high, low, and full. The low ranges from 4-14 kHz, the high ranges from 14-24 kHz, while the full setting ranges from 4-24 kHz. Using lower frequencies

reduces the attenuation of sound, allowing for greater penetration into the sub-bottom (up to 15 m). Since density changes are associated with changes in attenuation, however, a lower transmitting frequency reduces the system's ability to determine the boundaries of a density change (EdgeTech, 1996).

Methods

This study consisted of two major stages: data collection and data analysis. Three data sets were collected: sub-bottom profiler data, side-scan sonar data, and GPS navigational data. Once collected, the navigation data was merged with the sub-bottom and side-scan data so each of those sets could be analyzed. A bathymetric data set was also created from the sub-bottom data so the bottom surface topography could be studied.

Data collection proceeded in two phases. The initial search for the paleochannels was conducted within a large preliminary search area. This area was chosen based on the assumed position of the paleochannels from previous studies. Many tracks of data were collected over the search area (figure 4). The data collected, together with unpublished data collected by Clark (1996) and unpublished data collected by Kast (1997), were analyzed to determine the presence of any sub-bottom layers of importance. These were defined as layers of significant depth (more than 5 m) with well defined upper and lower boundaries. Such layers meet the criteria of the paleochannels found in other studies in different parts of the Chesapeake Bay. After locating important sub-bottom layering, detailed data was collected in the concentrated study area (figure 4).

The sub-bottom profiler data collection began in September of 1997, searching for the location of the Cape Charles paleochannel. This was accomplished by making multiple

north-south passes over the study area, concentrating on areas with multiple sub-bottom layers to narrow the search. Side-scan data collection began in November 1997. Sub-bottom profiler and side-scan sonar data were simultaneously collected over the Cape Charles paleochannel. In all, the Edgetech X-STARpc Full Spectrum Subbottom Profiler and EG&G Model 260-TH Side-Scan Sonar with digital tape storage collected nearly two dozen transects with approximately 150 km of sub-bottom and 90 km of side scan data.

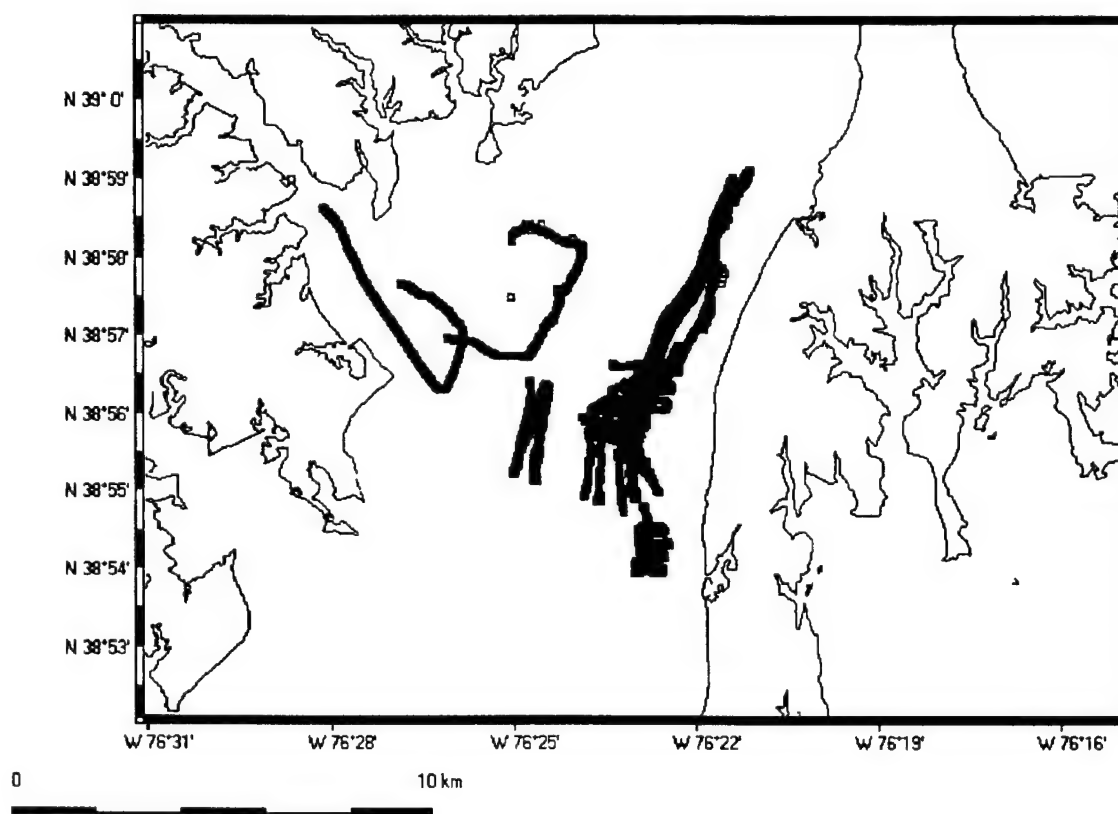


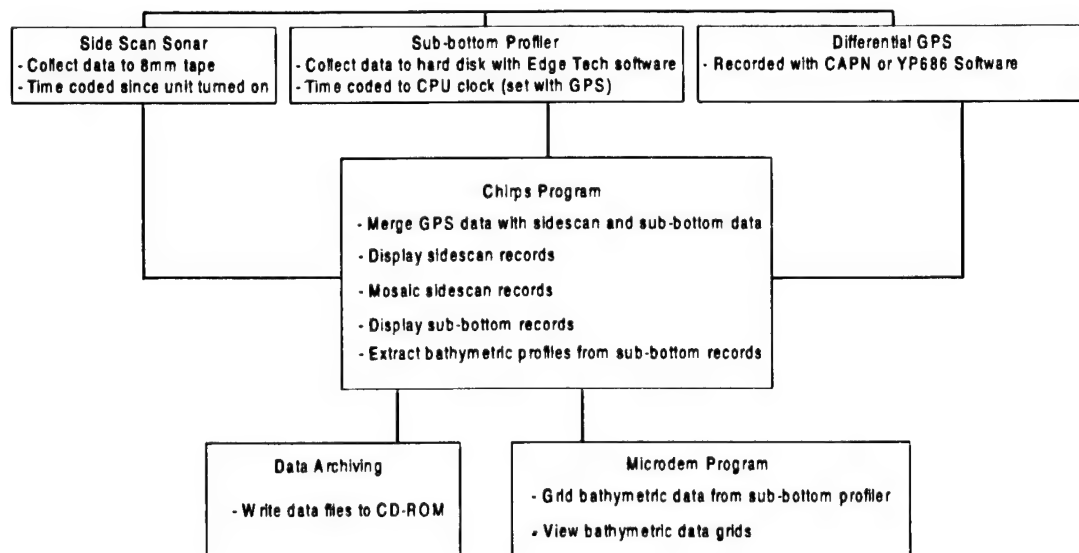
Figure 4 Preliminary search area and detailed study area. The preliminary search tracks are shown in black. The detailed search tracks are shown in red. The study area is the main area (red tracks) within the search area (black tracks) that contains significant layering in the sub-bottom.

Data Collection

Data were gathered using the EG&G Model 260-TH Image Correcting Side Scan Sonar, and the EdgeTech X-StarPC Full Spectrum Sub-Bottom Profiler, and Northstar

Differential Global Positioning System (DGPS) in conjunction with the U.S. Naval Academy's oceanography research vessel (YP-686). The equipment was scheduled four times a month from early September, 1997, until middle March, 1998. The sub-bottom profiler data were supplemented with data collected previously by Clark (1996) and Kast (1997).

Data Collection and Analysis



To collect side-scan data, the tow fish is towed in the water behind YP-686. The tow fish creates cross track profiles which are sent to the Model 260-TH Digital Correcting Side Scan Sonar via cable. The data are viewed on the paper printout of the Model 260-TH and a monitor and stored on an analog tape for review and processing at a later time. The tow fish does not have any type of positioning device, so the navigational data must be collected separately and then added to the side-scan data file.

The sub-bottom data are collected in a similar manner. However, to increase the ship's mobility and to avoid fouling the tow cables, the sub-bottom profiler is not towed behind YP-686. Instead, it is mounted on a steel frame and held in a fixed position along the starboard side of the research vessel. The sub-bottom profiler acts much like a depth sounder, creating a vertical profile of the area located directly beneath the sub-bottom profiler. During the data collection, the user can view the profile on screen, while the profile is saved to the XStar-PC's hard drive. The ship's navigational output is not compatible with the input interface for the Full Spectrum software, so the GPS data must be collected separately and then be added to the data file.

The CAP'N navigational software used aboard YP-686 collect position data for the side scan and sub-bottom, and overlays the location of the ship on a chart of the operations area, and continually updates the ship's position. The navigational data are loaded into the CAP'N program via a NEMA 183 output from the GPS receiver. A capture file was created to collect the GPS data from the NEMA 183 output (see Appendix A).

During post processing, the NEMA 183 capture file was converted to a format compatible with the sub-bottom and side-scan data files. The GPS times were then matched with the side scan sonar times to fix the position of the side scan data images. The GPS data were also matched with the sub-bottom data collection times to fix the position of the sub-bottom data images. (See Appendix B.)

Table 2 Collected Data Files.

File Name	File Type	Size	Transects?	Collected By
17oct96	Chirp	121,952KB		Clark
29oct96	Chirp	82,524KB		Clark
3feb97	Chirp	60,463KB		Kast
7apr97	Chirp	105,314KB		Kast
sub17apr	Chirp	57,102KB		Kast
25apr97	Chirp	85,421KB		Kast
28aug97	Chirp	87,468KB		Lopes
8sep97	Chirp	182,766KB		Lopes
15sep97	Chirp	116,472KB		Lopes
22sep97	Chirp	118,633KB		Lopes
29sep97	Chirp	17,944KB		Lopes
6oct971	Chirp	56,009KB		Lopes
6oct972	Chirp	63,831KB		Lopes
24oct97	Chirp	128,584KB		Lopes
27oct97	Chirp	150,752KB		Lopes
10nov97	Chirp	130,982KB		Lopes
17nov97	Chirp	66,343KB		Lopes
17bnov97	Chirp	87,419KB		Lopes
18nov97	Chirp	192,137KB		Lopes
18nov97	Side Scan	38,866KB		Lopes
19nov97	Chirp	137,001KB		Lopes
19nov97	Side Scan	49,768KB		Lopes
10dec97	Chirp	256,824KB		Lopes
26jan98	Chirp	223,645KB		Lopes
26jan98	Side Scan	48,964KB		Lopes
3feb98	Chirp	179,552KB		Lopes
3feb98	Side Scan	37,967KB		Lopes
18feb98	Chirp	194,470KB		Lopes
18feb98	Side Scan	43,543KB		Lopes
19feb98	Chirp	180,564KB		Lopes
19feb98	Side Scan	50,859KB		Lopes
2mar98	Chirp	225,072KB		Lopes
2mar98	Side Scan	50,081KB	A,B,C,D,E,F	Lopes
3mar98	Chirp	213,466KB		Lopes
4mar98	Chirp	193,108KB	X,Y,Z	Lopes
4mar98	Side Scan	41,529KB		Lopes
5mar98	Chirp	151,682KB		Lopes
5mar98	Side Scan	34,413KB		Lopes
16mar98	Chirp	227,829KB		Lopes
16mar98	Side Scan	31,979KB		Lopes

Data Analysis

The collected data (see Table 2) were viewed in a computer laboratory, using the software program "Chirps" (Guth, unpublished). This program allows the user to digitally process the data sets and subset small portions of each data set for detailed analysis. From the digitally processed data, several sub-bottom and side-scan images were selected for correlation and discussion.

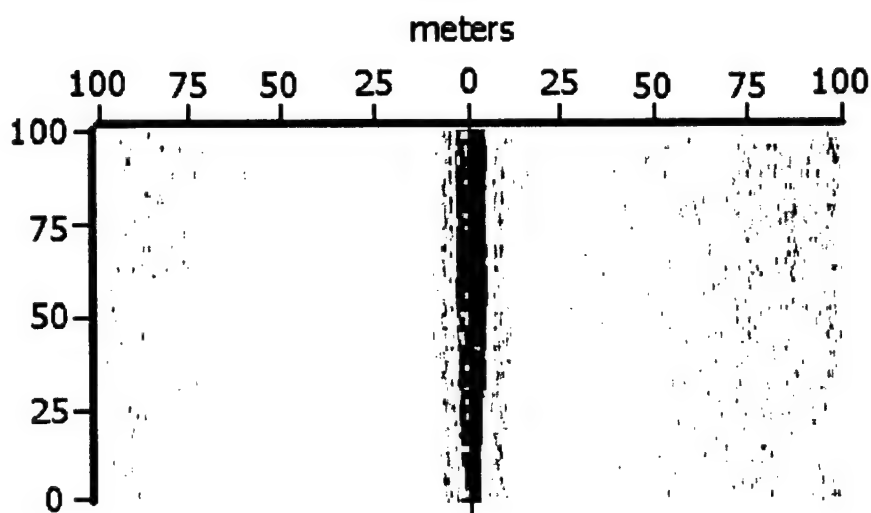


Figure 5 A typical side scan sonar sonograph. The dark vertical line referenced to 0 m indicates the ship's track (the course of the tow fish through the water). The horizontal distance is given in meters across the top, while the distance along the ship's track is given in the vertical axis in meters.

Side scan sonar data can be viewed in several ways. It can be displayed as a typical sonograph or as a mosaic. The sonograph resembles a graph. It has equal horizontal and vertical scales, achieved by omitting or redisplaying some of the horizontal rows of data, and shows the ship's track in the center of the image (see figure 5). This image has several features common to all sonographs. For the images discussed in this

study, white areas represent strong returns, while darker areas designate weak returns.

The vertical line down the middle of the sonograph designates the ship's track, or path of the tow fish. The horizontal range from the ship's track is given across the top of the image. For this study, a horizontal range of 100 m to either side was chosen. The distance traveled down the ship's actual course is given along the left side.

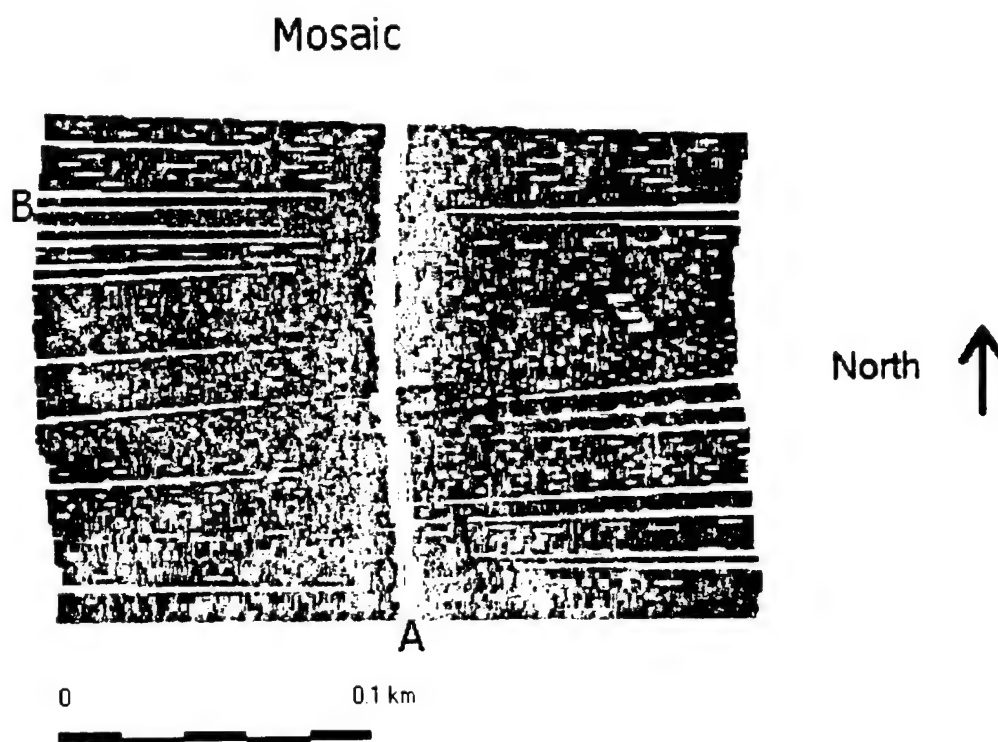


Figure 6 Side scan sonar mosaic. White line down the center of the mosaic (A) represents the ship's track. B shows the irregularities in the mosaic that arise due to small changes in the ship's course.

A mosaic displays the sonograph data on a chart, making it easier to see the exact location and orientation of the side scan sonar data (see figure 6). The white line down the center of the mosaic denotes the ship's track. The scale bar denotes the length and width of the mosaic. Irregularities in the mosaic arise due to small changes in the ship's

course. A small change in the course will skew the row of data collected at that instant, leading to duplicate collection of data over some points and missing data at other points. Interpolation of some of the data points helps fill in the missing data. Too much interpolation, however, averages out useful data.

The typical sub-bottom profiler image is significantly different than a side scan sonograph (compare figures 5 and 7). The vertical axis shows the depth below mean sea level in meters. The horizontal axis shows the chirp record number, which corresponds to the record's position within the file or horizontal distance. In some cases, the record numbers decrease from left to right across the horizontal axis, in order to place the western side of the image on the left side. The horizontal distance can be found using the CHIRPS software. But, as a rule of thumb, a typical ship's speed of 4 knots equates each record to approximately 0.30 meters (see Appendix C).

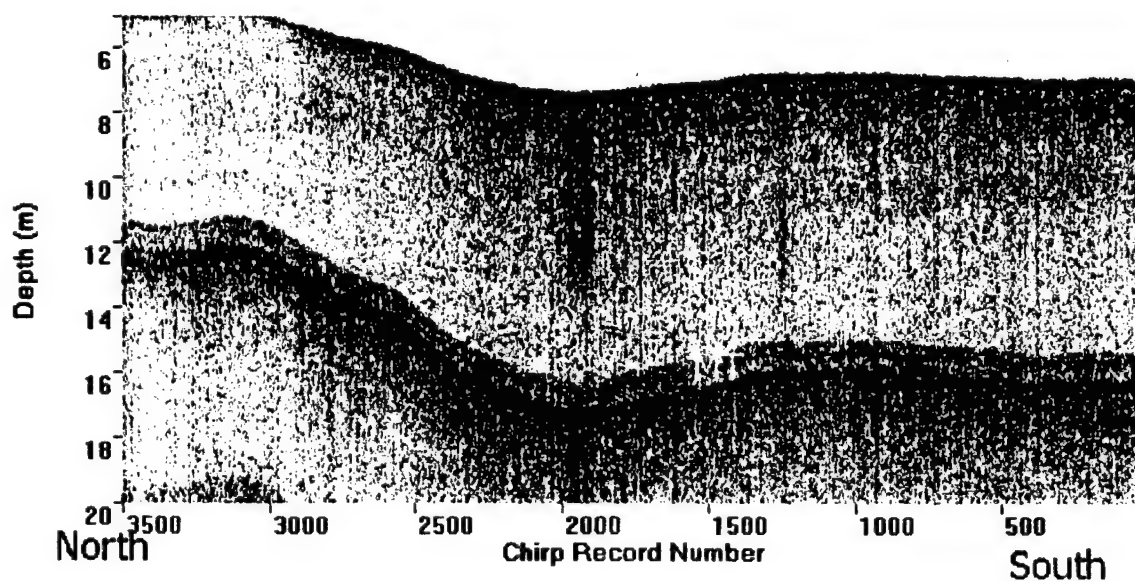


Figure 7 Typical sub-bottom profiler image. Image is from a north-south transect. MT represents a multiple return, not a sub-bottom layer.

The colors on the sub-bottom profile image represent the two bandwidths used.

By convention, subbottom profiler returns use black to show strong returns resulting from density contrasts, and show a single frequency. The Chirps program uses color to combine both frequency ranges, with green for the low frequency bandwidth (4 kHz – 14 kHz) and red the high frequency bandwidth (14 kHz – 24 kHz). Black signifies a strong return from each bandwidth. Yellow (the combination of red and green) signifies no return for either bandwidth. The color image superimposes both frequencies, highlighting where they differ (green and red colors) and where the two frequencies provide similar results (yellow and black colors). This differs from a conventional black and white image which shows either the low frequency, the high frequency, or a combined bandwidth, in shades of gray.

When analyzing a sub-bottom profile, it is important to take into account multiple returns (MT). The multiple returns appear as sub-bottom layering in the profile (see figure 7). However, they are located at twice the depth of bottom, and mirror changes in bottom bathymetry. They arise from transmitted sound energy that reflects off the bay floor, travels back to the surface where it is reflected back to the bottom and then returns to the sub-bottom profiler. This means that the sound energy of the multiple return has twice the TWTT as the sound energy from the bottom return. As a result, the multiples appear as sub-bottom layering located at twice the depth of the bottom. Since the TWTT is doubled any change in bottom surface bathymetry will be exaggerated in the multiple return. This means multiple returns appear in the sub-bottom profiler image as sub-bottom layers that mirror the bottom bathymetry with exaggerated slopes.

Results and Discussion

Subbottom Layering

Analysis of the sub-bottom data suggests the existence of several different channels near the eastern shore of the Northern Chesapeake Bay, located from N38 54.54' W076 22.81' to N38 58.98' W076 28.65'. These channels all have a North-South orientation. They are found at depths up to 14m below the sediment/water interface. Four layers can generally be resolved within the subbottom of the study area. From top to bottom, they will be referred to as layers I, II, III, and IV. Strong returns separate each layer, indicating a strong contrast in sediment properties (see figure 8). These strong returns are likely to represent erosional surfaces, with the lower layer being significantly more lithified.

Shallow layer I has an average thickness of 2m. It is characterized by smooth regular returns indicative of homogenous sediment. Intermediate layer II has an average thickness of 9m, and contains many distinct sub-bottom layers. Deep layer III has an average thickness of 3m and appears intermittently between layer II and IV. Layer IV extends below the strong return that marks the bottom of layer III. It also contains several strong returns, but is not well imaged due to limited return strength.

Locating the Paleochannels

Six transects (A-F) oriented in an east west direction, and three transects (Y-Z) oriented in a north south direction (see figure 9) clearly show the patterns of sub-bottom

layering. Figure 10 shows transect A. It bounds the northern end of the study area. The vertical axis is the depth in meters below sea level. The horizontal axis shows the chirp record number. The actual horizontal width of this figure is 300 m. Layer II running horizontally through the figure (depth of 2 m to 8 m below the bottom) is approximately 160 m wide. Layer III, with depths greater than 8 m below the bottom is the deepest layer visible for this image.

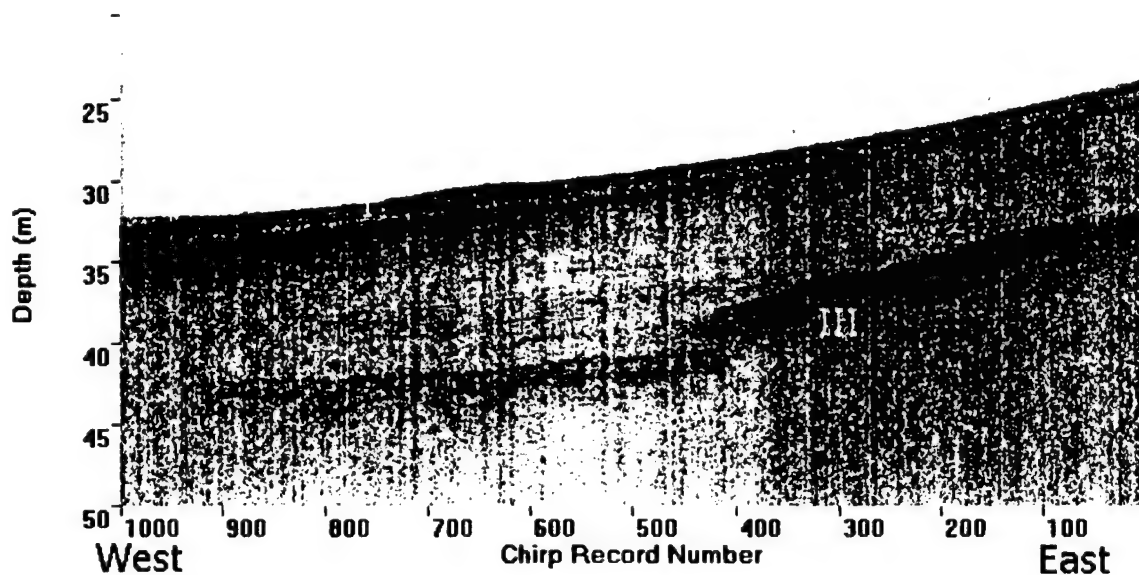


Figure 8 Transect B showing sub-bottom layers I, II, III, and IV.

Transect B, located approximately 600 m south south west of Transect A, is shown in figure 8. The shallow (I) and intermediate (II) layering are more clearly developed in this transect. It also appears that several deep layers exist. Layers I, II, and III in transect B are similar to that of the rest of the study area. However, there is another deep layer IV present. The intermediate layer II has a depth of 3 m to 10 m, and is characterized by many distinct returns showing internal sediment layers. Deep layer III has a depth of 8m to 10 m below the bottom. The deepest layer is separated from this

intermediate layer by strong returns nearly 14 m into the sub-bottom..

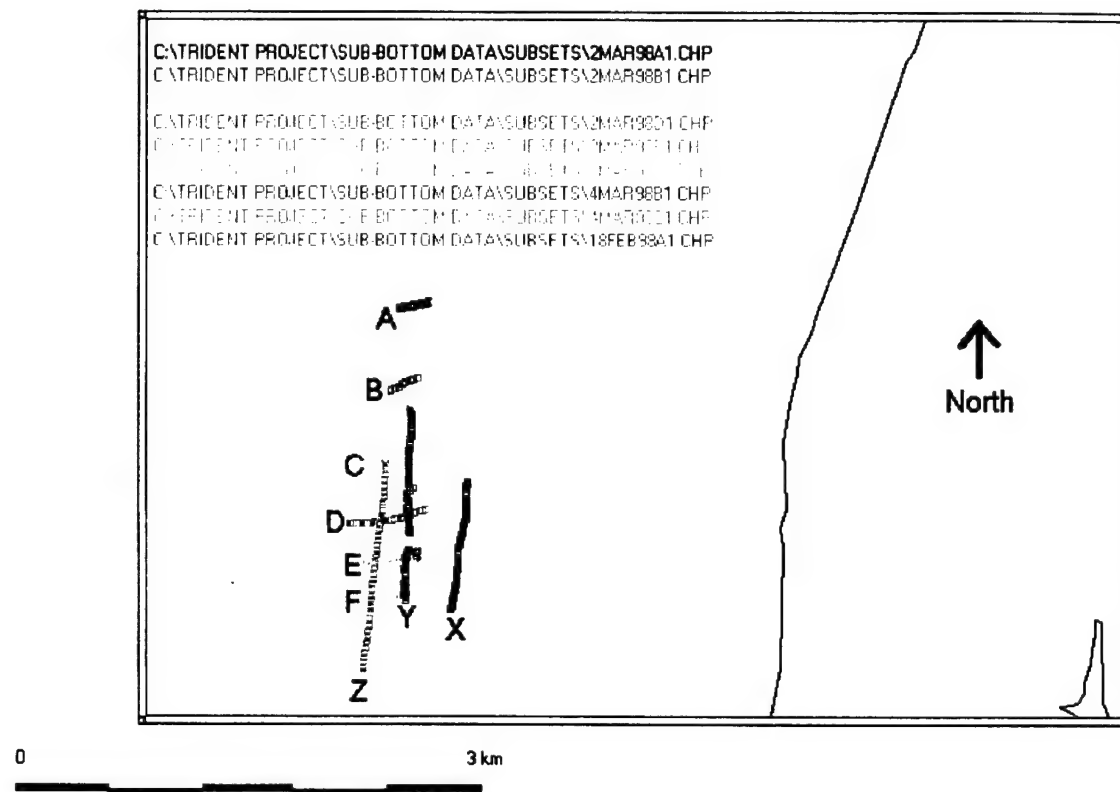


Figure 9 Chart showing the transects that identify and orient the deepest sub-bottom layering.

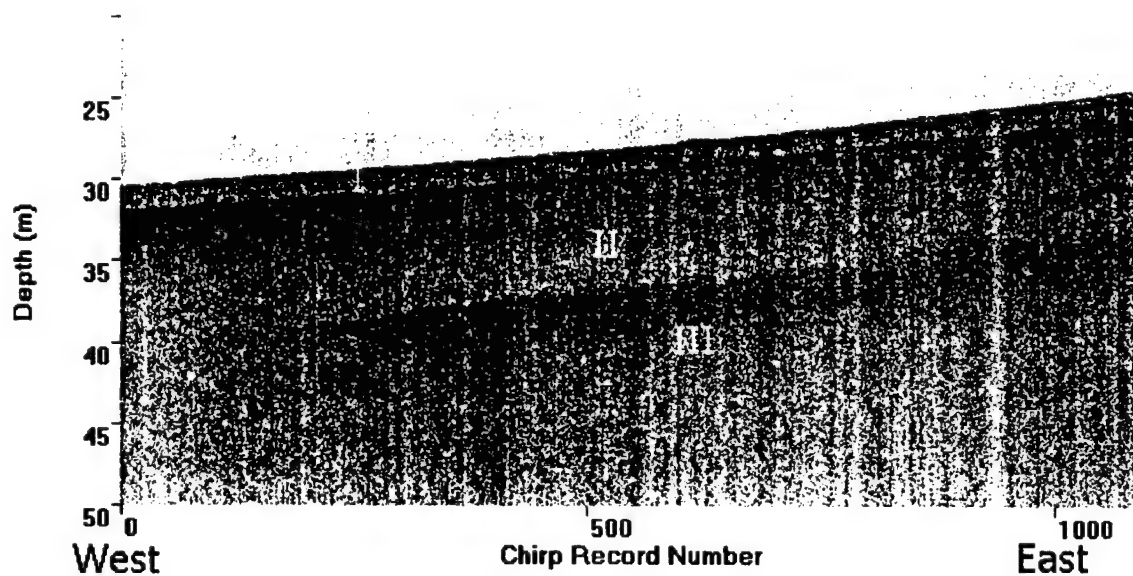


Figure 10 Transect A showing layers I, II, and III. Width of record approximately 300 m.

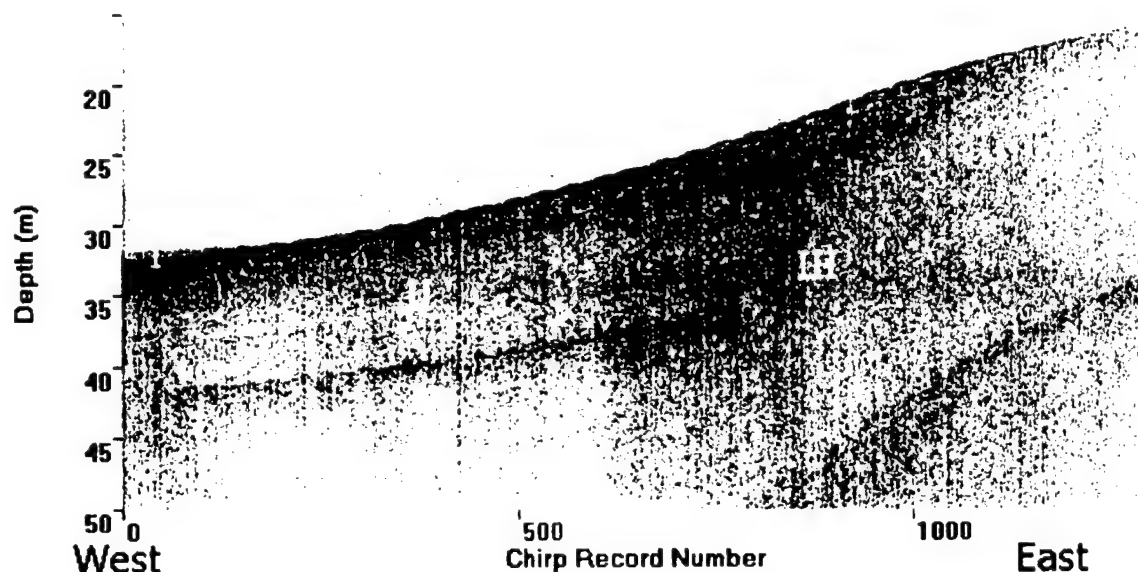


Figure 11 Transect C showing layers I, II, III, and IV.

This pattern of layering is repeated in transect C. Figure 11 shows the different layers in the sub-bottom profile from transect C. This transect is located approximately 500 m along a bearing of 170° from transect B. The width of the deep layer (IV) in transect C is 240 m. This is much longer than the deep layer (IV) from transect B, which is approximately 160m wide. The average depth of layer IV in transect B is 13 m. This is deeper by comparison than the average depth of 10 m in transect C (compare figures 8 and 11)

Examination of figure 12 shows that Layer III in transect D is not as wide, but deeper than the transect C. Layer IV from transect D is 180 m wide and averages 11 m in depth. In contrast, deep layer IV from transect C averages only 10 m (compare figures 11 and 12). Transect D is located approximately 270 m south of transect C on a bearing of 200° .

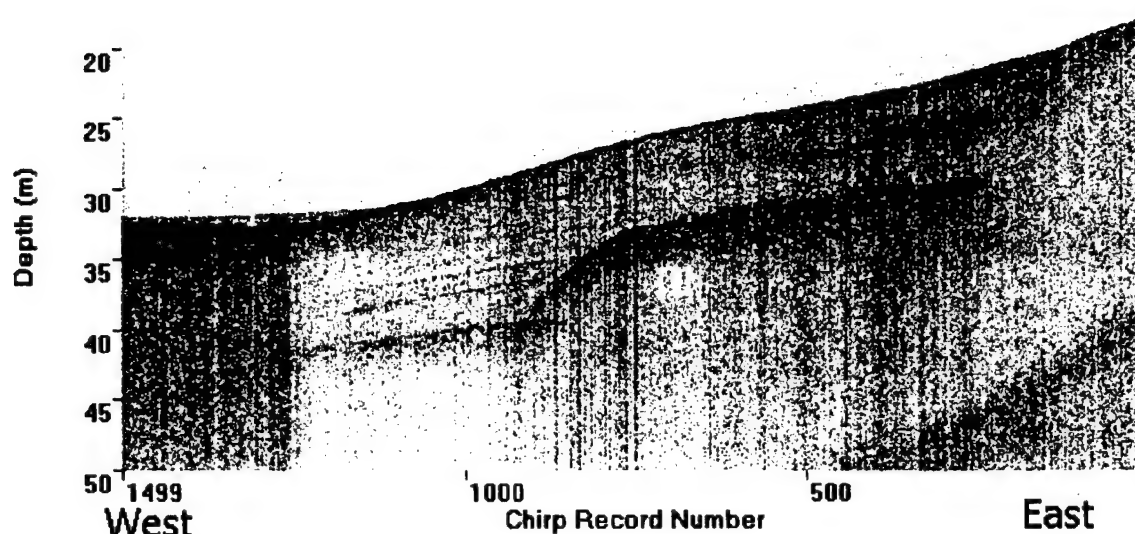


Figure 12 Transect D showing layers I, II, III, and IV.

Transect E (figure 13) provides the most interesting sub-bottom profile for the data set. This profile is located 250 m due south of the profile from transect D. The initial view of the profile suggests the deep layer (IV) is only 126 m wide, with an average depth of 11 m. However, close inspection reveals the deep layer probably runs the entire width of the figure. The deepest layer is 'blocked out' or masked in the middle of the figure by a stronger return from overlying intermediate layer III. Assuming that layer IV lies beneath the stronger return from layer III, the width of the deep layer becomes 325 m. With this assumption, the average depth of layer IV also increases to approximately 13 m.

Transect F is very similar to transect E (compare figures 13 and 14). Transect F is located 200 m due south of transect E. It has a strong layer III that masks a deeper layer IV. Assuming that layer IV runs beneath the strong return from layer III (like transect E), layer IV is 350 m wide. This is the widest point measured for layer IV.

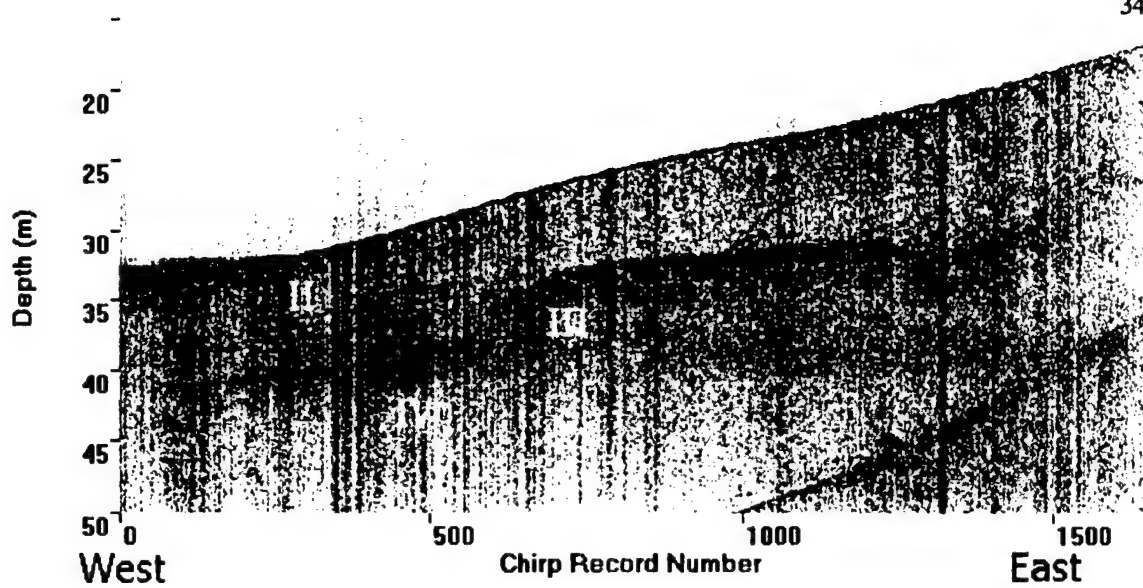


Figure 13 Transect E showing layers I, II, III, and IV.

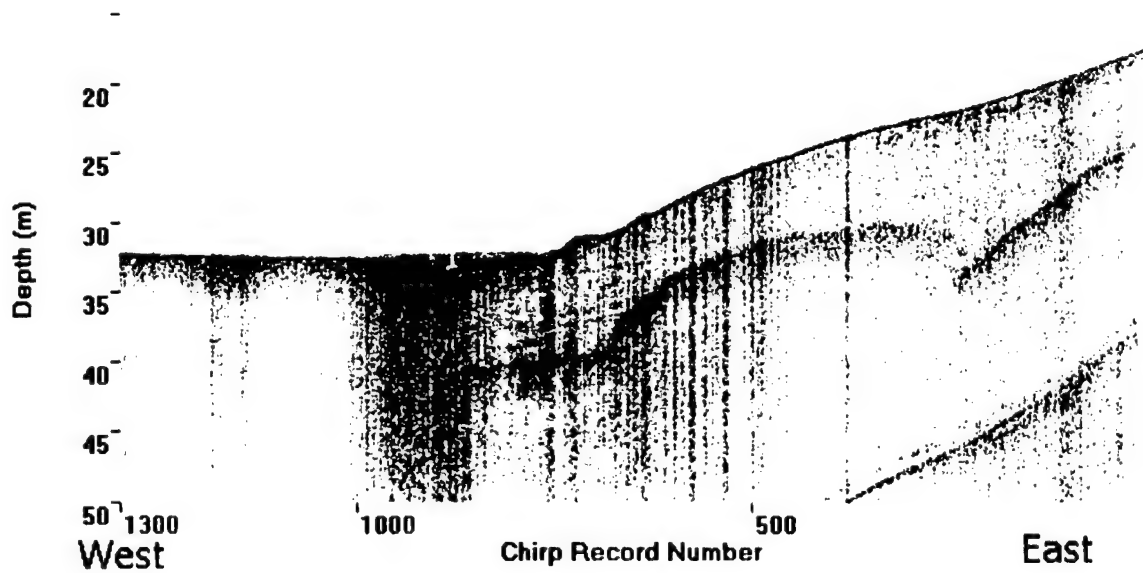


Figure 14 Transect F showing layers I, II, III, and IV.

The change in width of the sub-bottom layer is the most apparent difference between each of the six transects. It is also important to note that, in all of the profiles,

the depth of the sub-bottom layering tends to follow the bottom bathymetry. That is, as the depth of the water increases, so do the depths of the sub-bottom layers. Moving across the profiles from west to east shows the absolute depth of layer IV (the depth below mean sea level) decreases. At the same time, however, the depth of the layer below the bottom surface increases.

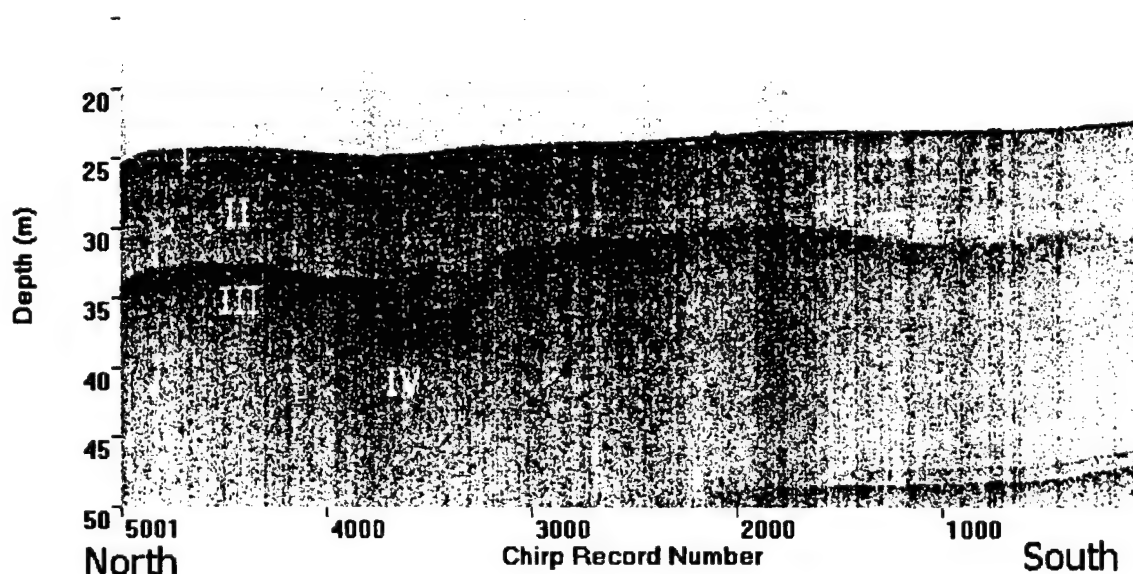


Figure 15 Transect Y showing layers I, II, III, IV, and the location of the channel 'C'.

Correlating the east west profiles with sub-bottom profiles in the north south direction shows the extent of the layering. Analysis of the data reveals the same deep layering in the east-west profiles. Figure 15 shows transect Y which is 1125 m long. Layer IV averages 13 m beneath the bottom. This section of the profile is shown in detail in figure 16. Careful inspection of the edges of layer IV in figure 16 shows that the deep layer clearly underlies the strong return from layer III. It is actually a channel cut in layer III that runs east-west and is 100 m wide.

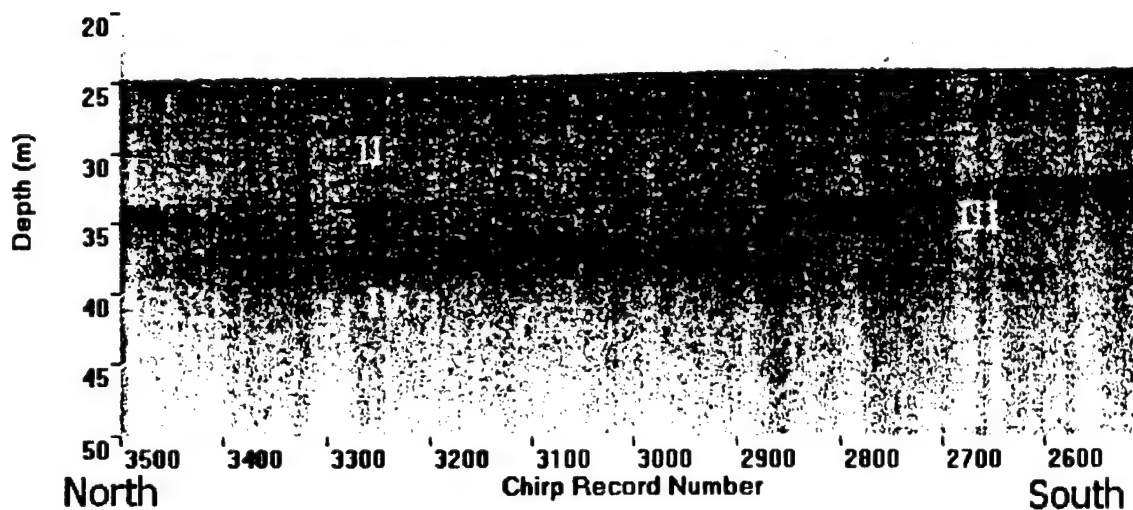


Figure 16 An enlarged view of the deep layer from transect Y. This shows layer IV clearly underlies layer III.

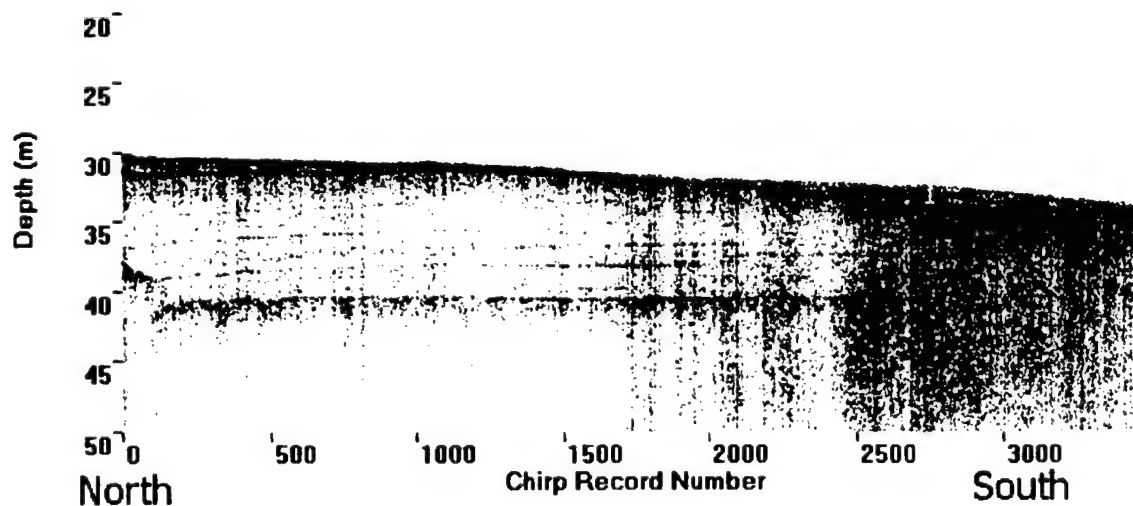


Figure 17 Transect Z showing layers I, II, III, and IV.

Transect Z is located approximately 150 m west of transect Y. The profile from this transect can be seen in figure 17. In this figure, layer IV is 1230 m long and has an average depth of 10 m. It is interesting to note that the layering at the southern edge of

transect fades into a dark area of strong but unresolved returns. Colman et al. (1990) suggest this type of profiling is a result of biogenic gas which results from degrading of plants and animals.

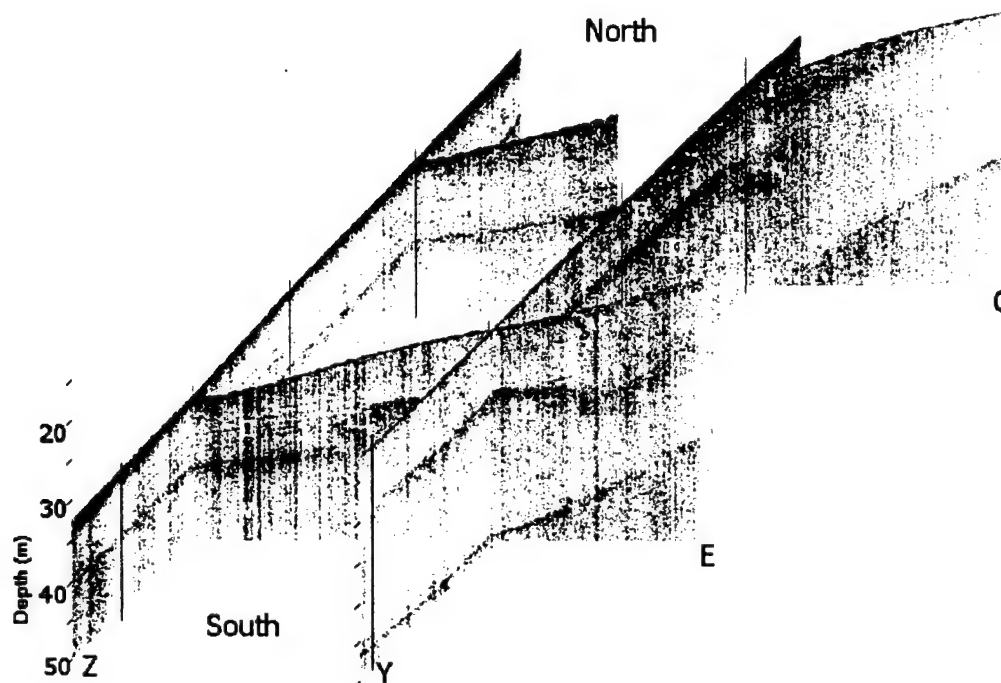


Figure 18 Transects C (blue) and E (green) cross with transects Z (skewed on the left) and Y (skewed on the right).

Orienting the Layering

To orient the layering, the east west transects (figures 8, 10 - 14) were pasted with the north-south transects (figures 15 - 17). Crossing the profiles where the data sets overlap produces a three dimensional view of the sub-bottom. Figure 18 shows the crossovers of the sub-bottom data tracks. It is easy to see layer IV is oriented in the north south direction. The deep layer slopes downward from east to west in the image, but

maintains a fairly constant slope in the north south direction. This would suggest that the layer may be the eastern boundary of an ancient river channel.

Classifying the Paleochannel

The north-south orientation of the deep layer suggests it follows the bathymetry of the main channel of the bay. Further, the Cape Charles paleochannel runs through the study area (Colman et al., 1990). The approximate position of the Cape Charles paleochannel (figure 1) suggests that its eastern edge is located near the center of the study area. It has already been established that the study area is located over the eastern edge of layers III and IV. Further, Colman et al. (1990) showed that the depths near the western edge of the Cape Charles paleochannel to be near 12 m below the bottom surface (see figure 19, which is about 100 km south of this study area). These depths are comparable to those of layer IV found in this study. Therefore, it is logical that the deep layer classified earlier is in fact the eastern edge of the Cape Charles paleochannel.

Comparison of figure 19 to transect Y (figures 15 and 16) helps determine the sediment layers present. Layers I and II, from transect Y, are sediments corresponding to the fill of the Cape Charles paleochannel. Layer IV is probably Tertiary sediments. There are two likely scenarios to explain the presence of layer III. In the first case, layer III is a previously unidentified tributary of an older paleochannel. The other likelihood is that layer III is an early stage of Cape Charles fill. The latter scenario is more probable since the Cape Charles paleochannel is the only channel previously identified in the study area.

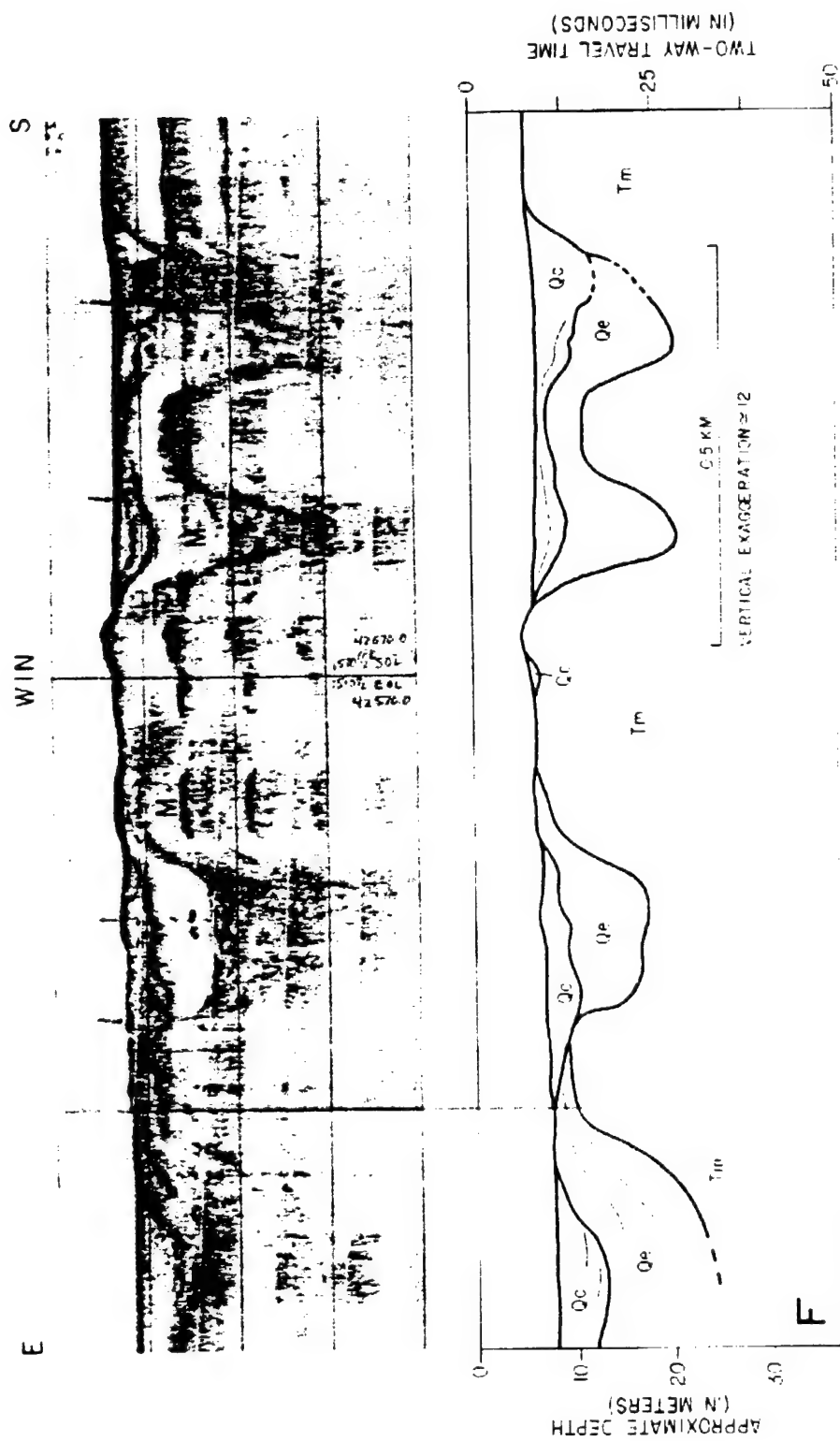


Figure 19 Sub-bottom profile of section F from Colman and Halk, 1989b.

Colman et al. (1990) categorized the paleochannel-fill sequences evident from sub-bottom profiling into two stages. The earlier stage (the lower layer) is characterized by strong, irregular, discontinuous reflections (Colman et al., 1990). The later stage (the upper layer) is characterized by weak, smooth, continuous reflections (Colman et al., 1990). Inspection of figure 18 shows that layer III has the characteristics described as the earlier stage of fill, while layers I and II have the same characteristics described as the later stage of fill. This supports the scenario that layer III is the early stage of Cape Charles paleochannel fill.

Bottom Bathymetry

The next objective of the study is to determine any correlation between the sub-bottom layering and the bottom bathymetry, to decide if different bedforms are indicative of sub-bottom layering. This was completed in two ways. First, the sub-bottom profiles were compared to a three-dimensional bathymetric map of the study area. Further, side scan sonar mosaics of the study area were analyzed to determine if any changes in bathymetry are too subtle for the bathymetric map.

A bathymetric map of the study area was created to compare to the sub-bottom layering. The computer program MICRODEM (Guth, 1995) was used to create a bathymetric grid of the study area. Using the depth of the bottom returns from applicable chirp records, MICRODEM creates a three dimensional view of the bottom surface (see figure 20). From this view (compare figures 20 and 21), it is evident that there are no bathymetric features that indicate the existence of sub-bottom layering. The comparison does show, however, that the sub-bottom layering tends to have the same orientation as

the bottom surface. That is the sub-bottom layering is oriented along the axial channel of the bay.

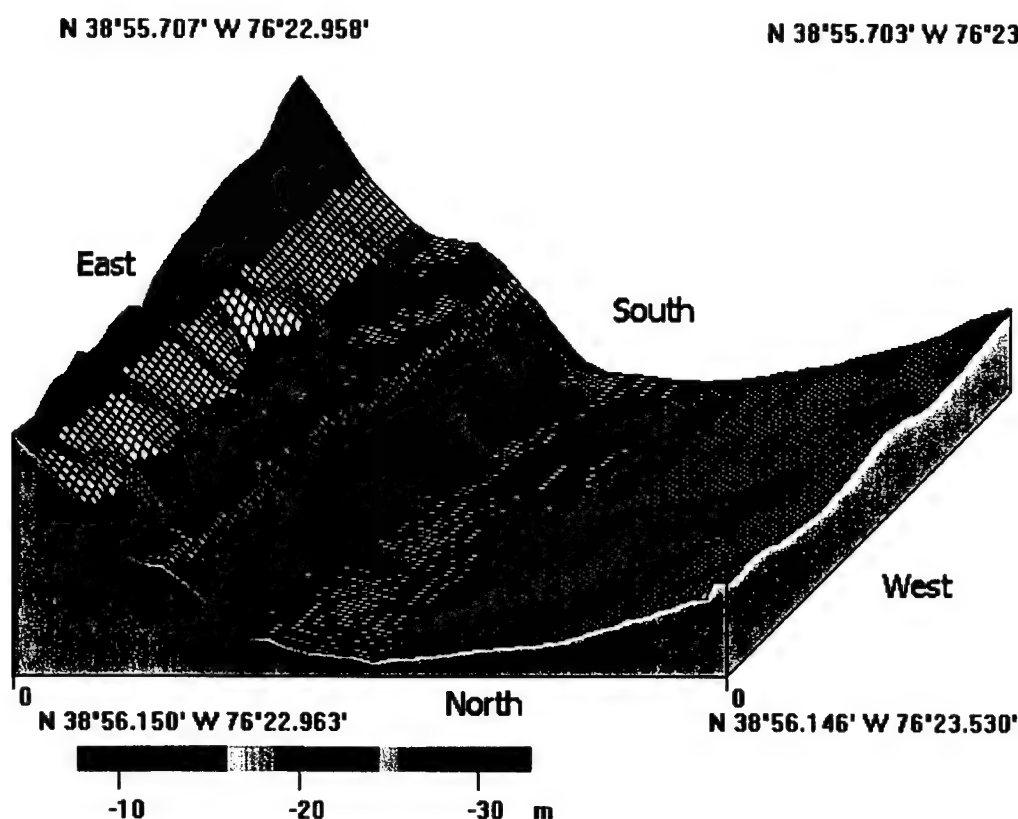


Figure 20 Bathymetric map of the study area. This map shows the changing bathymetry of the study area. The axial channel is in the center of the map, channel slopes up quite sharply towards the eastern shore, while it is a much more gradual slope up to the western shore.

To resolve the correlation between small bathymetric features and sub-bottom layers, side scan mosaics were compared with sub-bottom profiles. Side scan sonar mosaics and sub-bottom profiles were pasted together to correlate the data. Figure 22 shows a side scan mosaic matched with two crossover sub-bottom profiles. From this image, one can see that there are no indications of bedforms that correlate to the sub-bottom layering. There are no small bathymetric changes that relate to the presence of the

sub-bottom layering. Close examination of this image, however, shows some areas with markedly strong returns compared to the rest of the image. These areas of tonal patching and high acoustic energy return are indicative of rough surficial sediments (Circe and Escowitz, 1985).

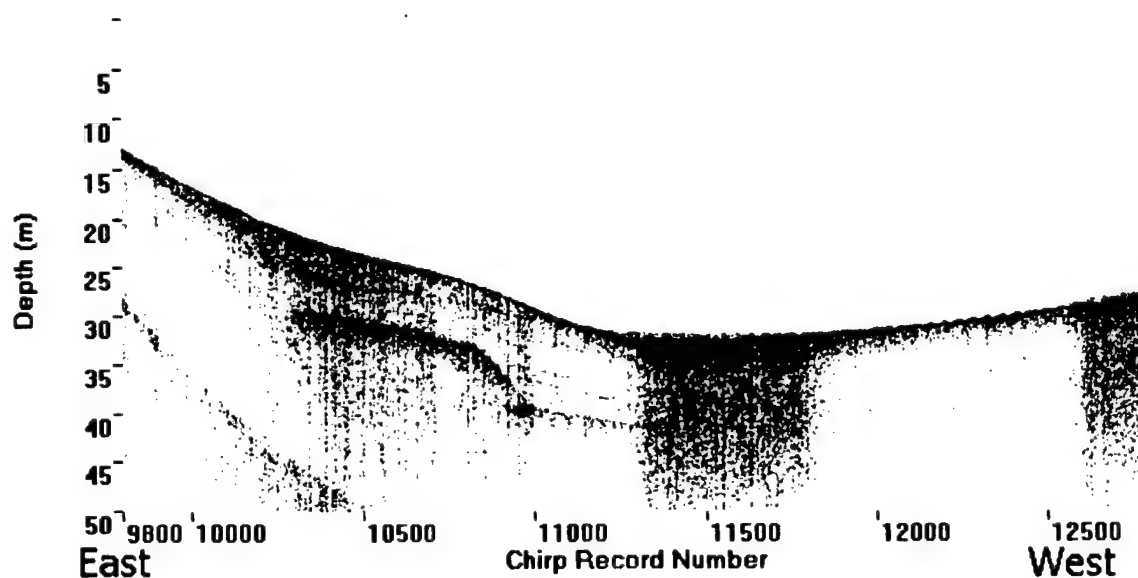


Figure 21 Sub-bottom profile across the northern edge of the bathymetric map. Reoriented to coincide with the view in Figure 20.

The side scan sonographs and sub-bottom profiles are related in one significant way. The tonal patching and high energy acoustic returns from the side scan sonographs coincide with the strong returns from the sub-bottom profiles. Comparison of the side scan mosaic with the sub-bottom profile taken along the same transect (see figure 23) clearly shows that the tonal patching and high energy returns from the sonograph appear with the strong returns in the sub-bottom profiles.

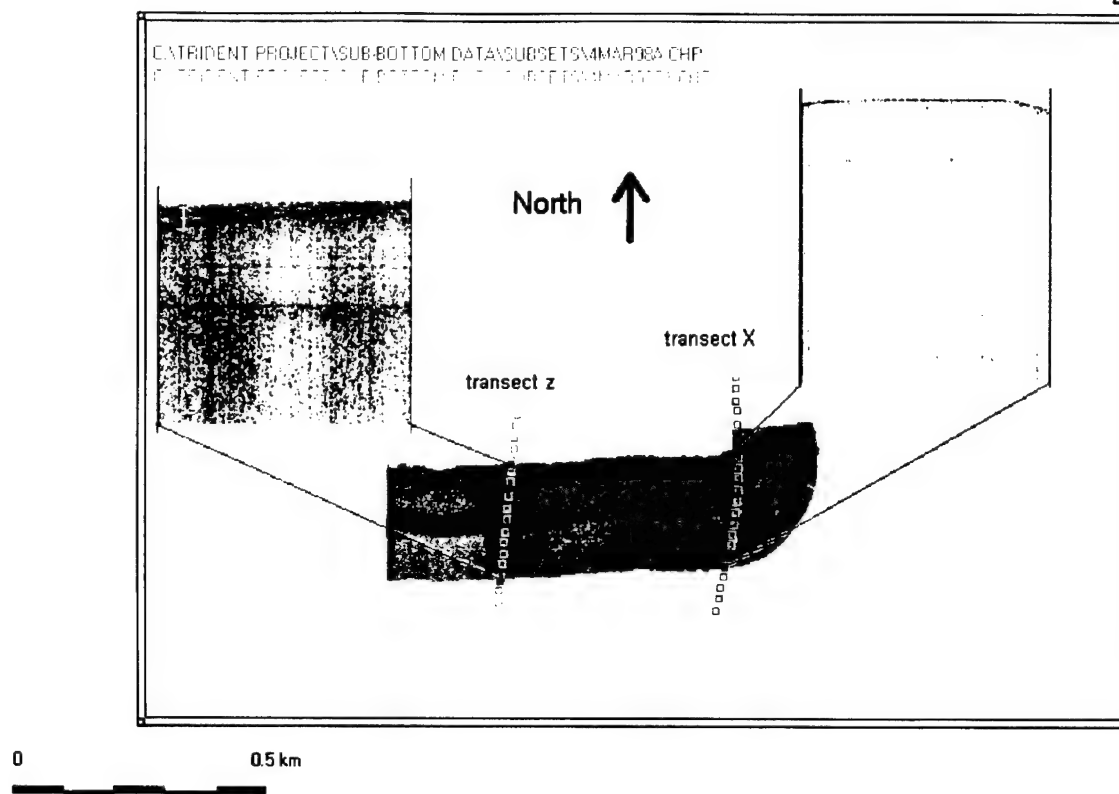


Figure 22 Side scan mosaic with two crossover sub-bottom profiles (transects X and Z).

Traditional side scan sonograph interpretation suggests that the areas of strong return are indicative of areas with rough surficial sediments. Areas where the soft sediments have been eroded away reveal hard, rough surficial sediments (Circe and Escowitz, 1985). The traditional sub-bottom profiler interpretation indicates that these areas in the sub-bottom contain biogenic gasses. The data suggests that tonal patching and areas of high acoustic energy return (changes in acoustic energy levels without changes in the bathymetry) from sonographs could be indicative of biogenic gas in the underlying sediments. There are several reasons for this theory.

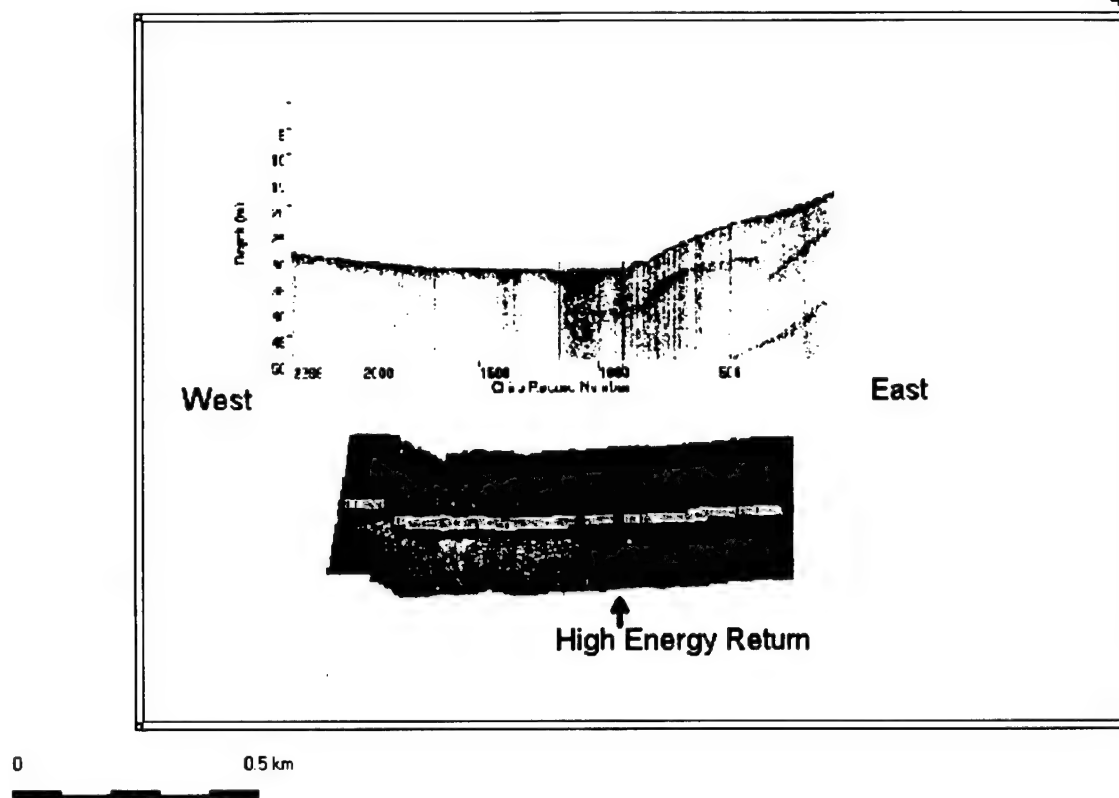


Figure 23 Side scan mosaic and concurrent sub-bottom profile. The two vertical blue lines on the sub-bottom profile correlate to the two blue marks on the side scan mosaic. The figure shows how biogenic gas (G) corresponds to areas of high side scan acoustic energy return.

Figure 23 clearly shows that the area of high acoustic energy return (side scan sonar) occurs in the same area as the biogenic gas (sub-bottom profiler). Further, the biogenic gas in figure 23 is located at the bottom of the axial channel in the Chesapeake Bay. This indicates that there are no currents or wind forces that might force the resuspension of the softer sediments leaving only hard coarse sediments in the area of the tonal patching. As a result, there must be some other causes for the high acoustic energy return evident in the side scan sonar data. The evidence suggests that biogenic gas is the most reasonable solution.

Sedimentation Rates

Locating the Cape Charles paleochannel was crucial to determining the sedimentation rate for the study area. The sedimentation rate (net buildup of sediments along the bay floor) was based on the depth of the Cape Charles paleochannel and its age. Since intermediate layer II is the eastern edge of the Cape Charles paleochannel, the age of the sediment at the boundary must be 18 ka (Colman et al., 1990). Dividing the average depth of the paleochannel from the sub-bottom data sets by the age of the channel gives an annual sedimentation rate.

A minimum depth of 9 m below the bottom surface and an age of 18,000 years yield a minimum sedimentation rate of 0.05 cm/yr. A maximum depth of 14 m and an age of 18,000 years give a maximum sedimentation rate of 0.078 cm/yr. An average depth of 10 m below the bottom surface and an age of 18000 years yield an average sedimentation rate of 0.056 cm/yr. This rate is slightly smaller than other sedimentation rates previously calculated. This is probably a result of slower sedimentation rates in the middle portion of the bay. Since the rate is calculated for such a long period of time, it averages all sediment types and flood events that may cause variations in sedimentation rates determined in other methods. Comparing this to a subsidence rate of 0.09 cm/yr (Nerem et al., 1998) suggests that there is a local increase in mean sea level.

Conclusions

Careful inspection of the sub-bottom data profiles shows the changing depth of the sub-bottom layering. The transects depict a deep layer overlain by an intermediate layer.

Intermediate layer II is located approximately 10 m below the bottom surface, while deep layer IV is located at depths greater than 14 m below the bottom surface.

Cross correlation of sub-bottom profiles oriented in different directions shows the ultimate orientation of the entire layer. The sub-bottom layering found in the study area is an ancient channel running along the axial channel of the Chesapeake Bay. The sediments were classified by comparing the location and depth of the four sub-bottom layers and their erosional surfaces to the paleochannels previously studied near the area. Layers I and II correspond to the late stage Cape Charles paleochannel sediment fill while layer III corresponds to the early stage Cape Charles paleochannel fill. Layer IV is probably Tertiary sediment.

For future study, there are two feasible solutions to support these conclusions. One method is to take core samples up to 10 m into the sub-bottom in the current study area. Then, classifying and dating the sediments for comparison to sediments of known age would resolve the age and origin of the sediments found in the sub-bottom layers. The other option is to continue collecting sub-bottom profiler data, heading south to a point that intersects with data from previous studies. Comparison of the sub-bottom profiles would then resolve any doubts to the origin of the layering.

Comparing sub-bottom profiles with bathymetric maps and side scan sonographs of the study area suggests that there is no relationship between sub-bottom layering and bathymetric features. The sub-bottom layers tend to have the same orientation as the existing bottom surface bathymetry. However, there is nothing to suggest that there are any bathymetric features that indicate sub-bottom layers must exist in the underlying

sediments. The one strong correlation is the appearance of high acoustic energy returns in accordance with strong sub-bottom profiler returns.

Traditionally, areas of high acoustic energy returns in side scan sonar data sets indicated the presence of hard or coarse sediments. The data suggests that the tonal patching and areas of high acoustic energy return indicate the presence of biogenic gas in the underlying sediment. This means that side scan sonar can be used to find biogenic gas deposits. Monitoring side scan sonar data for areas of high acoustic energy would indicate the presence of hard, coarse sediments or biogenic gas.

A simple sedimentation rate was calculated for the study area using the age and depth of the intermediate layer (II) in the study area classified as the Cape Charles paleochannel. This sedimentation rate of 0.056 cm/yr is slightly smaller than the sedimentation rates previously calculated for the entire bay. This is logical because sedimentation rates in the middle portion of the bay are lower than those in the upper and lower parts of the bay (Kerhin et al., 1988).

Comparison of the sedimentation rate to the subsidence rate for the area shows the net change in sea level is increasing. As a result, the addition of dredge spoils in the vicinity of the study area will not significantly damage the geologic structure of the northern Chesapeake Bay.

Naval Applications

The side scan sonar and sub-bottom profiler have many applications. Anti-Submarine Warfare and nautical mapping are two important naval applications of the

equipment. This study does not specifically target these applications. The methods employed in the data collection, however, readily apply to these missions.

Anti-Submarine Warfare is an ever increasing mission in the United States Navy (Douglass, 1996). A large part of ASW is the propagation of sound underwater. Since enemy submarines are detected mainly through the means of passive sonar, it is important to know the propagation paths of the sound emitted by the submarine (Gardner, 1996). Different sediment types have a large effect on the attenuation of sound waves when they reflect off the bottom. Sediment classification procedures can help determine different sediment types and their relative affects on sound. The tonal patching in the side-scan sonar records shows how the bottom surface characteristics affect the attenuation of the sound energy.

Nautical Mapping is a mission of the Navy's Meteorology and Oceanography community. The 'METOC' community is responsible to the Defense Mapping Agency (now the National Imagery and Mapping Agency) to provide the raw survey data to produce worldwide bathymetric charts (Davis, 1996). This study produced a bathymetric chart of the study area. Following similar procedures in other areas would allow remote sensing of the raw data needed to produce accurate bathymetric charts.

During the course of the study, these techniques were used to survey the route to the U.S. Naval Academy's hurricane anchorage. The sunken remains of an old railroad bridge, located in the Severn River just north of the U.S. Naval Academy Bridge, posed a possible navigational hazard to the Naval Academy's fleet of Yard Patrol Craft. The area was surveyed with the side scan sonar to remotely determine the geometric height of the

bridge ruins. Examination of the data showed that the ruins posed no threat to the Yard Patrol Craft. As a result, the route to the hurricane anchorage was shortened.

Acknowledgements

I thank QMC Russell and the crew of YP-686 for their cooperation. I thank Doug Smith and Kenneth Zepp for their technical advice and assistance. Paul Clark and Kelly Kast provided earlier sub-bottom profiler methods and Chris Linder provided side scan sonar methods. Peter L Guth advised and reviewed the entire project.

References Cited

- Bloom, A. L., 1983: Sea level and coastal changes. Late Quaternary environments of the United States, Volume 2, The Holocene. H.E. Wright, Ed., University of Minnesota Press, 42-51.
- Chen, Z. Q., C. H. Hobbs III, J. F. Wehmiller, and S. M. Kimball, 1995: Late Quaternary paleochannel systems on the continental shelf, south of the Chesapeake Bay entrance. *Journal of Coastal Research*, **11**(3), 605-614.
- Circe, R. C., and E. C. Escowitz, 1985: *Sidescan Sonograph Patterns Offshore of the Southern Delmarva Peninsula*. US Geological Survey, Open-File Report 90-662.
- Clark, P., 1996: Unpublished sub-bottom profiler data, midshipman research project.
- Colman, S. M., and J. P Halka 1989a: Quaternary geology of the southern Maryland part of the Chesapeake Bay: U.S. Geological Survey Miscellaneous Field Studies Map MF-1948-C.
- Colman, S. M., and J. P Halka 1989b: Quaternary geology of the southern Maryland part of the Chesapeake Bay: U.S. Geological Survey Miscellaneous Field Studies Map MF-1948-D.
- Colman, S. M., and C. H. Hobbs III, 1987a: Quaternary geology of the southern Maryland part of the Chesapeake Bay: U.S. Geological Survey Miscellaneous Field Studies Map MF-1948-A.
- Colman, S. M., and C. H. Hobbs 1987b: Quaternary geology of the southern Maryland part of the Chesapeake Bay: U.S. Geological Survey Miscellaneous Field Studies Map MF-1948-B.

- Colman, S. M., J. P Halka, C. H. Hobbs III, R. B. Mixon, and D. S. Foster, 1990: Ancient Channels of the Susquehanna River Beneath Chesapeake Bay and the Delmarva Peninsula. *Geological Society of America Bulletin*, **102**, 1268-1279.
- Cochran, J. K., 1984: Uranium and Thorium Decay Series Nuclides. *The Estuary as a Filter*. Victor S. Kennedy, Ed., Academic Press, 179-220.
- Davis, G. W., 1996: A new Naval Oceanography Policy. *Sea Technology*, **37** (January), 328-344.
- Dillon, W. P., and R. N. Oldale, 1978: Late Quaternary sea-level curve reinterpretation based on glaciotectionic influence. *Geology*, **6**, 56-60.
- Douglass, J. W., 1996: Undersea Warfare: Balancing Affordability and Advanced Technology. *Sea Technology*, **37** (January), 11-12.
- Dyer, K. R., 1986: *Coastal and Estuarine Sediment Dynamics*. John Wiley & Sons, 342pp.
- EdgeTech, 1996: *X-StarPC Full Spectrum Sub-Bottom Profiler Technical Manual*.
- EG&G Marine Instruments, 1990: *Model 272-TD Dual Frequency Tow Fish with TVG*.
- EG&G Marine Instruments, 1991: *Model 260-TH Image Correcting Side Scan Sonar*.
- Gardner, W. J. R., 1996: *Anti-Submarine Warfare*. Brassey's, 160pp.
- Gross, M. G., M. Karweit, W. B. Cronin, and J. R. Schubel, 1978: Suspended sediment discharge of the Susquehanna River to northern Chesapeake Bay. *Estuaries*, **1**, 2, 106-110.
- Guth, P.L., 1995, Slope and aspect calculations on gridded digital elevation models: Examples from a geomorphometric toolbox for personal computers: *Zeitschrift fur*

Geomorphologie N.F. Supplementband 101, 31-52.

- Helz, G. R., S. A. Sinex, G. H. Setlock, and A. Y. Cantillo, 1981: Chesapeake Bay sediment trace elements. Research in Aquatic Geochemistry Report, Department of Chemistry, University of Maryland, 202pp.
- Hill, J. M., and J. P. Halka, 1989: *IGC Field Trip 231: Bottom Sediments of the Chesapeake Bay: Physical and Geochemical Characteristics*. 28th International Geological Congress. American Geological Union, 20pp.
- Hobbs, C. H., 1986: Side-Scan Sonar as a Tool for Mapping Spatial Variations in Sediment Type. *Geo-Marine Letters*, **5**, 241-245.
- Kast, K., 1997: Unpublished sub-bottom profiler data, midshipman research project.
- Kerhin, R. T., J. P. Halka, D. V. Wells, E. L. Hennessee, P. J. Blakeslee, N. Zoltan, and R. H. Cuthbertson, 1988: *The Surficial Sediments of Chesapeake Bay, Maryland: Physical Characteristics and Sediment Budget*. Maryland Geological Survey, no. 48, 82pp.
- Kerhin, R. T., J. P. Halka, D. V. Wells, E. L. Hennessee, P. J. Blakeslee, N. Zoltan, and R. H. Cuthbertson, 1982: Physical characteristics and sediment budget for bottom sediments in the Maryland portion of the Chesapeake Bay. Final draft report from Maryland Geological Survey to Chesapeake Bay Program, Environmental Protection Agency, 190pp.
- LeBlanc, Lester R., 1992: Marine Sediment Classification Using the Chirp Sonar. *Journal of the Acoustical Society of America*, **91**, 102-115.

- Nerem, R. S. et al., 1998: Chesapeake Bay Subsidence Monitored as Wetlands Loss Continues. *EOS*, **79**, 12, 149-157.
- Oertel, G. F., and A. M. Foyle, 1995: Drainage displacement by sea-level fluctuation at the outer margin of the Chesapeake Seaway. *Journal of Coastal Research*, **11**(3), 583-604.
- Officer, Charles B. et al., 1984: Chesapeake Bay Sedimentation Rates. *The Estuary as a Filter*, Victor S. Kennedy, Ed., Academic Press, 131-157.
- Reed IV, T.B., and D. Hussong, 1989: Digital image processing techniques for enhancement and classification of SeaMARC II side scan sonar imagery. *Journal of Geophysical Research*, **94**, B6, 7469-7490.
- Schock, S. G., and L. R. LeBlanc, 1990: Chirp Sonar: New Technology for Subbottom Profiling. *Sea Technology*, Sept, 35-43.
- Schock, S. G., L. R. LeBlanc, and L. A. Mayer, 1989: Chirp subbottom profiler for quantitative sediment analysis. *Physics*, **54**, 4, 445-450.
- Symonds, Philip, and Peter Davies, 1986: Deep-Tow Side Scan Sonar. *BMR Research Newsletter*.
- U.S. Army Corps of Engineers, 1998: *Potential Open Water Placement of Dredged Material at Site 104*. Site 104 Newsletter, Issue 2.
- Zabawa, Christopher Franc, 1978: *Flocculation in the Turbidity Maximum of Northern Chesapeake Bay*. UMI Dissertation Services, 123pp.

APPENDIX A: Using Cap'n Navigation Program

The Cap'n navigation program is a commercial navigation program with instant tracking. It uses a GPS input to continuously plot the ship's current position and course. This program is used extensively aboard YP-686. The following steps delineate how to capture the NEMA output from the GPS and save it to a computer file. (NEMA is the format of the GPS output for computer input.)

Capturing the NEMA input with the program open and running:

- Open a capture file for the GPS NEMA input before side-scan sonar and sub-bottom profiler data acquisition begins.
- With the Cap'n program setup and running, right click on the position window.
- Select 'Open Capture File'.
- Enter the name of the file (*.log).
- End the data capture when side-scan sonar and sub-bottom profiler data acquisition is complete.
- Right click on the position window.
- Select 'Close Capture File'.
- The capture file is then saved to the computer's hard disk.

APPENDIX B: Using Chirps

Written by Assoc. Prof. P. L. Guth, Oceanography Dept., USNA, the chirps program allows the user to view and manipulate side-scan sonar data and sub-bottom profiler data. The following outlines the most efficient way to prepare both data types for use with the CHIRPS software.

1. Sub-bottom profiler data

- While collecting, write Sub-bottom data to the hard disk on the XStar-PC, save as *.seg.
- Using CHIRPS convert the captured navigation file from the CAP'N program (*.log) to the format compatible with the sub-bottom profiler data file, save as *.gps.
- Add the new navigation file (*.gps) to the sub-bottom profiler data file using CHIRPS, save as *.chp.
- For ease of use and transportation, write the new data file (*.chp) to a CD using a writeable CD-ROM drive.
- Subset useful portions of the sub-bottom data file using CHIRPS to simplify the analysis.

2. Side-scan sonar data

- While collecting, write the side-scan data to an 8mm tape using the EG&G Model 260-TH Image Correcting Side Scan Sonar and Model 300 digital tape.

- On several occasions during the data collection period, record the time difference between the GPS receiver and the EG&G time (which starts at 0:00:00 when it is turned on).
- Transfer the 8mm data file to a DOS file using the NOVA software utility (See Appendix D) and save as *.egg.
- For ease of movement write the data file (*.egg) to a CD using a writeable CD-ROM drive.
- Add the converted navigation data (*.gps) to the side-scan data file using CHIRPS, save as *.egg (Note: when adding the navigation data, the user must enter the time difference between the GPS time and the EG&G time recorded during data collection).
- Subset useful portions of the side-scan data file using CHIRPS to simplify the analysis.

APPENDIX C: Useful CHIRPS Information

File (Program) Menu:

- Open Chirp Record – Opens a Chirp data file for viewing.
- Open Side Scan Record – Opens a Side Scan data file for viewing
- Mosaic Side Scan – Creates a mosaic (aerial view) of a side scan data file
- Chirp Data Manipulation
 - Subset New File – allows the user to select and save a portion of a large data file to a new file; saves all the records within the specified range
 - Thin New File – allows user to make the specified file smaller by choosing to save every n^{th} record
 - Add Navigation Data – allows the user to add GPS position data to an existing sub-bottom data file
 - Convert Old File – converts a data file made with the original XStar-PC program to the new format
- Side Scan Data Manipulation
 - Add Navigation Data – allows the user to add GPS position data to an existing side scan data file
 - Subset Data – Allows the user to select and save a portion of a data set as a new file.
- GPS Data Manipulation

- Convert NEMA 183 File – use this option to convert the NEMA 183 capture file (*.log) to the format compatible (*.gps) with the sub-bottom and side-scan data files
- GPS File → ASCII – translates the converted NEMA file (*.gps) into an ASCII file
- Close – closes all windows and exists CHIRPS

2. File (Map) Menu (displayed when the Map is the active window):

- Print – prints the current map projection
- Save – saves the current map projection as a bitmap
- Edit – allows the user to edit the current map projection before saving it as a bitmap
- Load – loads a saved BMP for comparison
- Setup Printer Image – creates a map for printer output or slide show
- Close – closes the map projection window

3. Calculate Menu (displayed when the Map is the active window):

- Bearing – calculates the bearing between two points on the data display
- Distance – calculates the distance between two points on the data display

4. Modify Menu (displayed when the Map is the active window):

- New projection – allows the user to select new map projection parameters
- Graphical resize – select a region to change the map display
- Zoom In – allows the user to zoom in on a selected portion of the projection
- Zoom Out – allows the user to zoom out to view a larger portion of the projection

- Move NW Corner – allows the viewer to view a different portion of the projection in the window with the same scale
 - Mouse – allows this option to be completed with the mouse
 - Keyboard – allows this option to be completed with the keyboard
- Outline Coast – allows the user to load a coast outline
- Point Locations – allows the user to open and display a file containing specific points
- KM Scale – displays a kilometer scale bar on the projection; length varies with map area
- Key Latitudes – displays key latitudes on the map (equator, tropics, and polar circles)
- Force Redrawing – redraws the original projection (i.e. before it was modified)
- Restore Projection – allows the user to display a new map projection
- Save Projection – saves the current map projection
- Coordinates – allows the user to select the units used when displaying coordinates
 - Degrees – selects degrees (i.e. 36.3456°)
 - Minutes – selects minutes (i.e. $36^{\circ} 23.1'$)
 - Seconds – selects seconds (i.e. $36^{\circ} 23' 1.26''$)

5. File (Graph) Menu (displayed when the data file is the active window):

- Print – allows the user to print the current data graph
- Save Image – allows the user to save the current data graph

- Edit Image – allows the user to edit the current data graph before saving it as a bitmap
 - Close – closes the current data graph
6. Rescale (displayed when the data file is the active window):
7. Analyze (displayed when the data file is the active window):
8. Overlay Menu:
- Text Labels – allows the user to add a text label to a specific point on the projection
 - Outline – overlays an outline onto the current projection
 - GPS – displays NEMA 183 navigation data as it is fed into the computer in real time
 - Replay GPS – allows the user to open and display a saved GPS navigation file (*.gps)
9. View Menu:
- Chirps Record – allows the user to view the return strengths of various chirp records
 - Single – allows the user to view the return strength of a single record as function of depth
 - All – allows the user to view the return strength of all of the chirp records in a file
 - New File – allows the user to display a new data file
 - Sidescan Record – allows the user to view the return strength of a sidescan record

- Chirp Record Locations – displays the locations of the records in a specified sub-bottom data file
- Sidescan Record Locations – displays the locations of the records in a specified sidescan data file
- Depth Map – display's a map showing the depth and location of the records in a chirp data file

10. Options Menu:

- Linear – uses linear scaling to display 32767 values to 255 shades of gray
- Log – uses logarithmic scaling to display 32767 values to 255 shades of gray
- Bottom Return Value – allows the user to set the minimum return value for the bottom on chirps data files; used to avoid returns within the water column
- Chirps – allows the user to set the parameters for viewing a sub-bottom data file (low frequency, high frequency, combined, and reverse display)
- Sidescan Tow distance – allows the user to input the distance at which the sidescan sonar was towed; needed for mosaics

11. Window

- Cascade – arranges the open windows in a cascade fashion
- Tile – arranges the open windows in a tile fashion
- Select – allows the user to select any open window as the active window

12. Help

- Contents – allows the user to access the help files

- **Hardware** – shows information about the current hardware setup
- **About** - shows version, copyright and author information

APPENDIX D: Using NOVA Software

The NOVA software utility is a commercial software utility for use with 8mm data tapes.

The following instructions show how to use the NOVA software utility to convert an 8mm data tape file to a DOS file.

- At the DOS prompt type: DAT=9
- At the DOS prompt type: EXABYTE=9
- Execute the TPU.EXE program file
- Select 'Copy Tape File to DOS'
- Type in the following parameters:
 - Filename: *.egg
 - Files to Copy: 1
 - None
 - Fixed
 - Block Length: 1800
 - Record Length: 1800, 0, ALL
 - 0
 - Fixed